ZYGO WIDE-FIELD INTERFERENCE OBJECTIVE DESIGN

by

Nathaniel S. Austin

_____

A Thesis Submitted to the Faculty of the

COLLEGE OF OPTICAL SCIENCES

In Partial Fulfillment of the Requirements

For the Degree of

MASTER OF SCIENCE

In the Graduate College

THE UNIVERSITY OF ARIZONA

2023

THE UNIVERSITY OF ARIZONA
GRADUATE COLLEGE

As members of the Master's Committee, we certify that we have read the thesis prepared by **Nathaniel Austin**, titled *ZWF and Michelson 1x Interference Objective Design* and recommend that it be accepted as fulfilling the thesis requirement for the Master's Degree.

_____   Date: 8/18/2023
Professor Brandon D. Chalifoux

_____   Date: 08/18/2023
Professor José M. Sasián

_____   Date: 08/18/2023
Daniel A. Russano

Final approval and acceptance of this thesis is contingent upon the candidate's submission of the final copies of the thesis to the Graduate College.

I hereby certify that I have read this thesis prepared under my direction and recommend that it be accepted as fulfilling the Master's requirement.

_____   Date: 8/18/2023
Professor Brandon D. Chalifoux
Master's Thesis Committee Chair
Wyant College of Optical Sciences

2

Acknowledgements

The author would like to acknowledge the following for their contributions:

Land Acknowledgement

We respectfully acknowledge the University of Arizona is on the land and territories of Indigenous peoples. Today, Arizona is home to 22 federally recognized tribes, with Tucson being home to the O'odham and the Yaqui. Committed to diversity and inclusion, the University strives to build sustainable relationships with sovereign Native Nations and Indigenous communities through education offerings, partnerships, and community service.

Dedication

For my wife, Kate – It's thanks to your love and support (and patience) that I was able to realize this dream. On to the next adventure!

For my cat, Hunny Badger – *Slow blinks*

8

Figures

11

13

14

Tables

Abstract

In this paper we discuss elements of optomechanical design as they relate to the design of a 1x Zygo Wide-Field (ZWF) interference objective, focusing on the design process and considerations. We review details on the motivation for many of the system requirements. We stress understanding the optimization operands that compose the merit function used to optimize the nominal design. We discuss tolerance operands and stress structuring the tolerance scheme to replicate the physical motion of optics as they are constrained by the mechanics. We then detail several relevant alignment methods that may be used and stress identifying the mounting method for proper tolerancing. We then go into detail on the interference cell, which is a critical component of the interference objective.

17

1. Introduction

1.a. Coherence Scanning Interferometry

In applications that require high precision control of surface topography and texture, a high precision metrology solution is paramount. coherence Scanning Interferometry (CSI) is the preferred method of areal surface topography due to the extremely high precision of the CSI measurement method, the non-contact measurement, high spatial resolution, areal surface coverage, and commercial availability of CSI metrology systems. This type of tool is referred to as a 3D optical profiler (or sometimes white light interference microscope).

Figure 1: High end 3D Optical Profiler from Zygo[i]

The 3D optical profiler system is like an optical microscope in that it consists of a removeable, infinity-corrected objective installed onto a profiler head. A schematic of the optical layout is shown in Figure 2; the items numbers from that figure are included in this section for clarity. The tube lens (130) within the profiler head images the object under test onto the detector plane (140). There are serval notable differences, however, between an optical microscope and an optical profiler. The interference objective (110) must have an additional interference cavity (112, 113) to create the necessary fringes that are measured to

---

[i] https://www.zygo.com/products/metrology-systems/3d-optical-profilers/nexview-nx2

create the height map of the surface. The profiler head must provide some modulation (170) of the cavity so that the fringes are not static on the detector. This may be achieved by precisely moving the entire objective relative to the surface under test (120) via e.g., piezoelectric transducers (150) referred to as a scanner. And finally, the resulting data captured from the scan must be rapidly analyzed by a computer (not shown) to produce the resulting 3D phase map representing the topography of the surface under test. The operator may then further analyze the phase map in software, such as Zygo Mx.
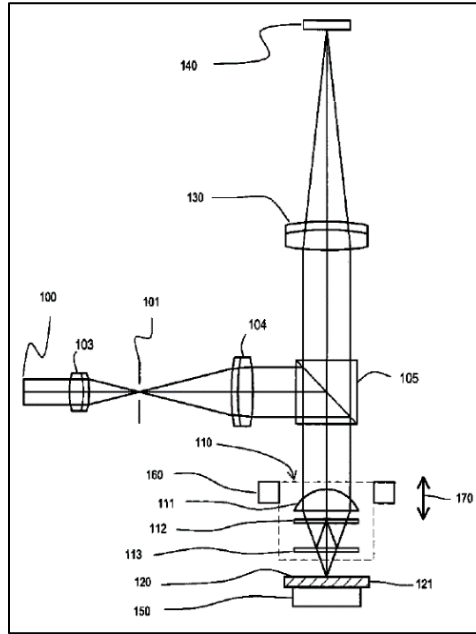
Figure 2: Schematic of CSI 3D optical profiler with Mirau-type objective

1.b. Design Goals

This paper will focus on the design of an interference microscope objective mentioned in the previous section. We will largely ignore the function of the profiler head other than where it is necessary to understand the requirements of the objective or where additional context will aid the discussion.

The purpose is to provide a feasible toleranced optical design of a patented Wide-Field (ZWF) objective type. The specifics of this objective type and comparisons to Mirau and Michelson objectives are discussed in section 1.d. We focus on low-NA, wide-field applications for which this design excels.

19

We discuss considerations for a more optomechanical design process throughout. The goal is to integrate understanding and consideration for mechanical mounting configurations into the tolerancing process to reduce design cycles. We will also demonstrate other basic optomechanical analysis on the most critical components to ensure design feasibility.

1.c. CSI Operating Principles

Because the objective we will discuss is to be used with a CSI optical profiler, it is important to understand the operating principles of the system. The Coherence Scanning Interferometer has been called the Scanning White-Light Interferometer, though this term has fallen out of use with the International Organization for Standardization (ISO) in favor of the more general term. This naming convention alludes to the broadband nature of the illumination source. Due to the broad band source, the CSI method has a very short coherence length. Compare the few-micron coherence envelope (Figure 4) typical of a white light source, to the >100 m coherence length of a stabilized HeNe laser Fizeau interferometer.
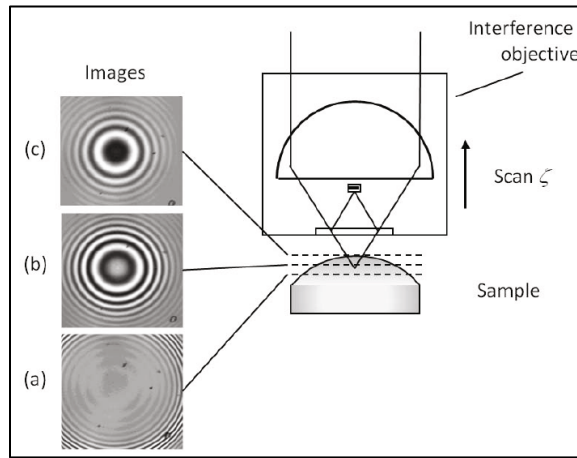
Figure 3: Diagram showing coherence envelope as seen by 3D optical profiler as interference objective scans spherical sample. (1)

20
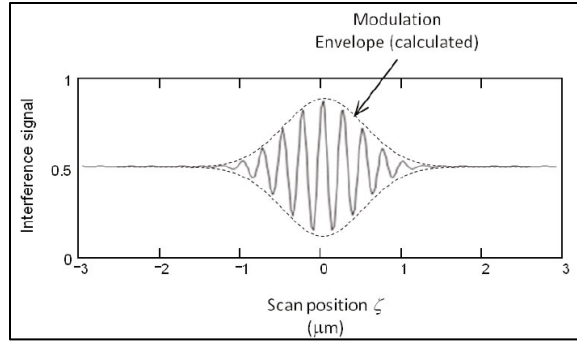
Figure 4: Interference signal vs scan position demonstrating modulation envelope. (1)

The interference cavity requires a Beamsplitter surface and a reference surface. Due to the short coherence length in objective cavity, the test surface must be positioned such that the Optical Path Difference (OPD) between the test leg and reference leg is near-zero. More precisely, the OPD must be smaller than the coherence envelope. When these conditions are met, the two beams interfere, and fringes are observed. When the test piece is within the coherence envelope and fringes are observed, they must then be modulated. The entire objective is scanned so that the coherence envelope passes entirely through each point within the field, or at least the desired test area.

1.d. Interference Objectives

There are three types of interference microscope objective that are available in the Zygo Optical Profiler Accessories catalog: Michelson, Mirau, and Zygo Wide-Field (ZWF). If we limit ourselves to this set of objective types, we can leverage the institutional knowledge that exists at Zygo. This knowledge can include design principles, manufacturing methods, and a mature supply chain. Using already established product lines may also help with customer acceptance when the product is released for sale.

Interference objectives contain imaging optics as well as an interference cell. The interference cell contains the Beamsplitter and Reference optics and generally defines the appropriate use-cases. We will compare the relative benefits of the 3 objective types mentioned above in the following sections.

d.1. *Michelson Objective*

The Michelson objective utilizes a Non-Polarizing Beamsplitter (NPBS) cube to split the test and reference leg into orthogonal directions. Because the objective is telecentric in object

21

space, the NPBS cube face must be strictly larger than the Field of View (FoV) of the objective. Therefore, the volume, mass, and (roughly) the cost of the NPBS cube increases with the *cube* of the FoV. The size and weight of the mechanics within the reference arm also increase correspondingly. The overall weight of the objective can be a limiting factor with the precision scanners used in high-end 3D optical profilers.

The test leg is transmitted straight through and exits the objective into object space. The reference leg is reflected at 90 degrees toward the reference flat, typically a Silicon Carbide flat or similar. The reference flat must be well aligned to the optical axis of the objective (after reflection from the cube) and so also requires a complex arrangement of mounting and alignment hardware in the reference leg of the objective. Because the reference leg is perpendicular to the test leg, all of this (the NPBS cube, reference mirror, reference mirror mounting/alignment fixturing, and a protective housing) hangs off the side of the objective. This creates a long cantilever and significantly reduces the resonant frequency of the objective.

The size and weight of the cube and this perpendicular geometry set a practical limit on the field size of commercially viable objectives. While a 1x Michelson objective is feasible; Zygo offers a 1x Long-Working Distance Michelson and a 1x Super-long Working Distance Michelson. However, there is significant customer demand for a more compact 1x interference objective, such as the ZWF, that would mitigate those issues, to justify developing a potential design.
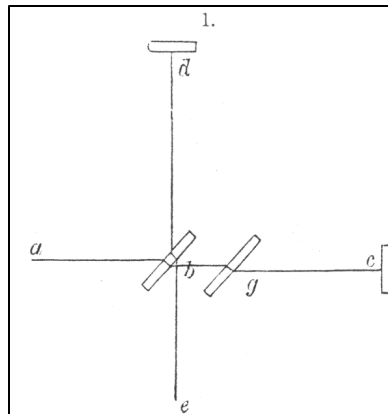
Figure 5: Pencil Diagram of Michelson Interferometer. This original implementation uses a plate beamsplitter and a compensatory plate of similar thickness. (2)

22
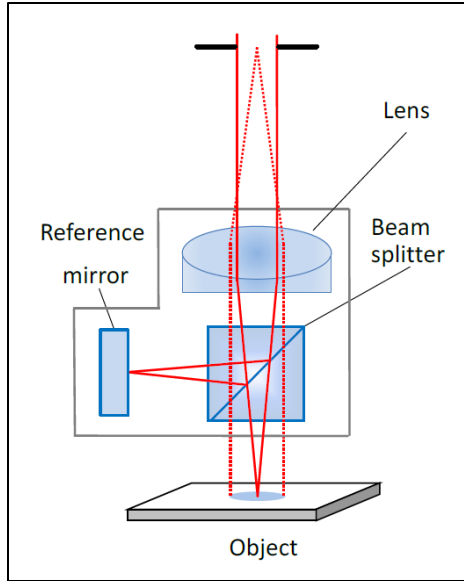
Figure 6: Diagram of Michelson interference microscope objective. (3)

d.2. *Mirau Objective*

The Mirau uses a pair of plane-parallel plates to provide the Beamsplitter and Reference surfaces. The plates are positioned normal to the optical axis of the objective. The bottom plate acts as the Beamsplitter. Again, the test leg is transmitted through the Beamsplitter out the front of the objective to the surface under test, however, the reference leg is reflected directly back toward the incoming beam. The Reference plate is located at the internal image plate of this reflected path. See Figure 7.
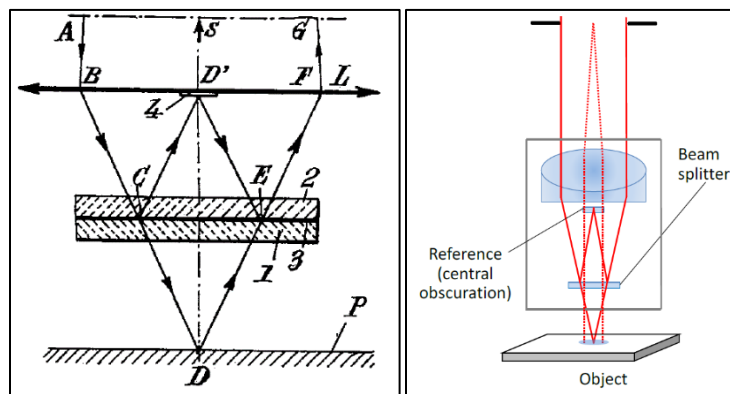
Figure 7: 2 diagrams of Mirau interference objective. Mirau's figure from Patent US2612074 (left), and a more modern figure with central obscuration and illumination beam (right). (3)

The reference surface needs to be optically thick (T = 0) to prevent any transmitted light, which would be directed toward the detector. The central obscuration created by the

reference spot is at least as large as the FoV, so this configuration is limited to high-NA, high Mag objectives where the obscuration is a relatively small fraction of the imaging cone at the reference surface. Specifically, the NA should be large enough such that the imaging cone of every field point contains the reference obscuration. This objective type is therefore not viable at 1x magnification.

d.3. *Linnik*

For completeness, we'll also mention the Linnik interference objective. In this configuration, the beam is split by an NPBS cube like a Michelson. However, instead of a single imaging lens located before the cube, there is a lens in each of the test and reference legs. This configuration does not need to accommodate any interferometer components after the imaging lens, so the WD is maintained. This can be useful for very high NA applications that would be limited by the Mirau configuration. However, with both imaging lenses within the interferometric cavity, it is extremely sensitive to alignment and both lenses need to be well matched for adequate dispersion. For lower NA applications, this configuration would quickly grow to an unwieldy size, so it's not viable for 1x objective.
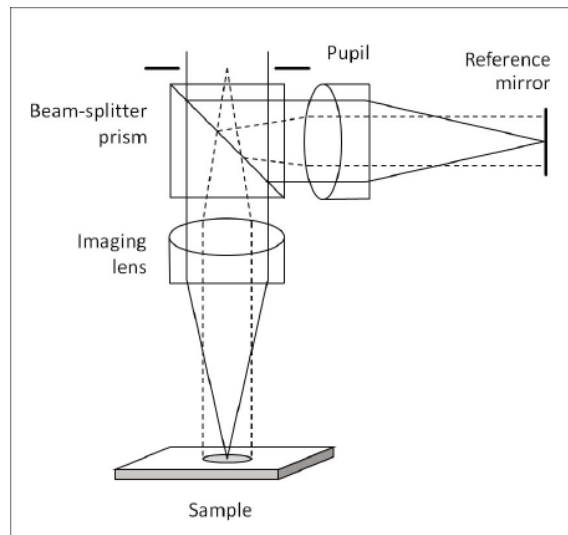
Figure 8: Linnik-type Interference Objective. (4)

d.4. *Zygo Wide-Field (ZWF)*

A relatively new type of interference objective is the patented Zygo Wide-Field (ZWF). The design overcomes the limitations of both the Michelson and Mirau objective types. The ZWF utilizes plane parallel plates in a (nearly) axial configuration to act as the Beamsplitter

and reference surfaces. The reference and Beamsplitter plates are tilted with respect to the optical axis so any light transmitted through the reference surface will be blocked by the aperture stop. This configuration requires that the BS plate be tilted by *at least* the NA of the objective and the Ref plate must be tilted exactly twice as much as the BS.

The ZWF offers significant benefits over the Mirau and Michelson objectives for low NA, wide-field applications. As mentioned in section d.2, the Mirau is not suitable for low-NA applications. The ZWF rejects any light passing through the Reference plate, so the Reference plate does not need to be optically thick and there is no central obscuration. This mitigates the limitation for low NA objectives. This is a significant improvement over Michelson objectives in wide-field applications because the NPBS cube is removed. The ZWF plates can be lighter than an NPBS for a Michelson with an equivalent FoV by roughly a factor of 4, not to mention the weight of the reference mirror and additional mechanics. Reducing load on the scanner may facilitate even higher precision scanners. And finally, without the reference leg cantilever, the objective will be more stable in noisy customer environments.
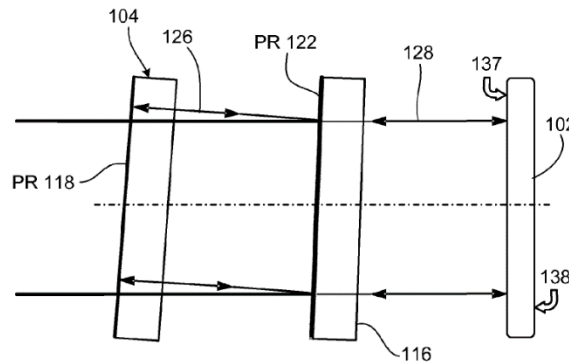
Figure 9: Figure showing beam path within ZWF interference cavity. The Beamsplitter plate is tilted so that reflected light is rejected by the system stop and the Reference plate is tilted at twice the BS angle. [ii]

[ii] Patent US 8,045,175
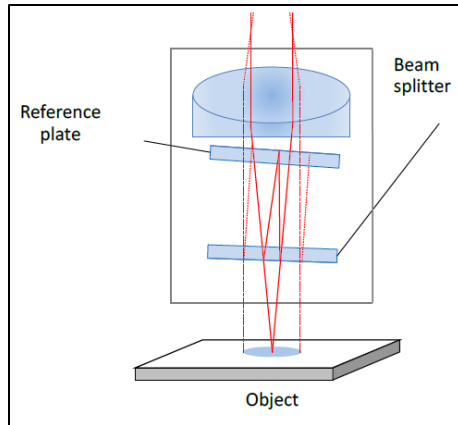
Figure 10: Diagram of ZWF interference microscope objective. (3)

There is a practical limitation to the ZWF objective type, which is set by the NA of the objective. The entire imaging cone must be blocked by the system stop, so the tilt of the BS plate must be larger than the NA of the objective, and the Ref plate tilt would be twice that. A high magnification objective with a large NA cannot accommodate the necessary plate tilt.

This makes the ZWF an excellent choice for low-NA, wide-field interference objective applications.

1.e. Optomechanical Design Process Overview

The general optical design process is outlined below, summarized from Field Guide to Lens Design (5) and modified to include a focus on integrating optomechanical considerations into the optical design process.

1. Establish Product Requirement Document; 2
2. Determine Appropriate Design Form; 3.a
3. Identify Design Starting Point; 3.b
4. Create Merit Function; APPENDIX A
5. Optimize Nominal Design; APPENDIX B
6. Create Tolerance Table; 5.b
7. Tolerance As-Built Performance; 0
8. Define Mounting Configuration; 6.b, 6.c
9. Define Compensators; 6.f
10. Define Critical Assembly and Alignment Requirements; 7.c
11. Define Optical Test methods and Validation Requirements; 8

26

These sections also go into detail on general considerations that an optomechanical designer should be aware of, that have a specific application to this design, or both. Many optical designers in industry work in cross-functional teams along with mechanical engineers and designers. The goal of this discussion is to understand mechanical requirements such as mounting tolerances to improve communication within the design team and to reduce design cycle time.

2. Design Requirements

2.a. Product Requirements Introduction

Before beginning an optical design, the design parameters must be defined. In this section we first give the product requirements table, then we go on to discuss the provenance of each as well as how we plan to achieve each within the optical design software package. We'll be using Zemax for discussion and demonstration, but other commercially available lens design packages have similar functionality. Details on the Optimization Operands mentioned that are used in Zemax Merit Function Editor (MFE) can be found in APPENDIX A.

In practice, some compromises may be made during the design phase that alter these parameters. A compromise might include the reducing performance goal to allow for loosened (or merely achievable) tolerances and therefore meet cost targets.

2.b. Product Requirements Table

Table 1: Design Parameters and Requirements

Sect.	Lens Parameter	Requirements
2.c	Wavelength Range	475-675 nm
2.c	Primary Wavelength	540 nm
2.d	EFFL	200 mm, Nominal
2.e	Parfocal Distance	120 mm, Nominal
2.f	Working Distance	>10 mm required; >12 mm goal
2.g	Numerical Aperture	0.03
2.g	Field Angle/Field Number (FN)	3.6° for FN 25
0	Optical performance	Diffraction Limited at 1x system mag
2.j	Distortion goal	< 0.1%
2.k	Lateral Color	< 0.25 pixel
2.l	Telecentric Object Space	
2.n	Temperature Range	15° C to 30° C; Operating -20° C to 50° C; Shipping
2.o	Optimum Sample Reflectivity	Fused Silica, 3.5%
7.e.3	Resonant Frequency	> 200 Hz

2.c. Wavelength Range

From the Product Requirement Table, we see the wavelength range is listed as 475 – 675 nm, however, this does not fully describe the illumination spectrum. In many imaging optical systems, the input illumination may not be exactly known. For example, for a camera the subject may be illuminated by any number of lighting conditions; Direct sunlight, artificial lamps, or low-light conditions. In these cases, it is best to design across the entire visible spectrum.

For the case of this objective, the illumination profile is defined by the instrument on which it will in used, which is well-known for the Zygo Optical Profilers on which this objective is intended to be used. Figure 11 shows that the illumination spectrum peaks in the green light and tapers off toward the ends of the spectrum. Within the optical model, we will use the illumination spectrum to weight our wavelengths according to their relative intensity.
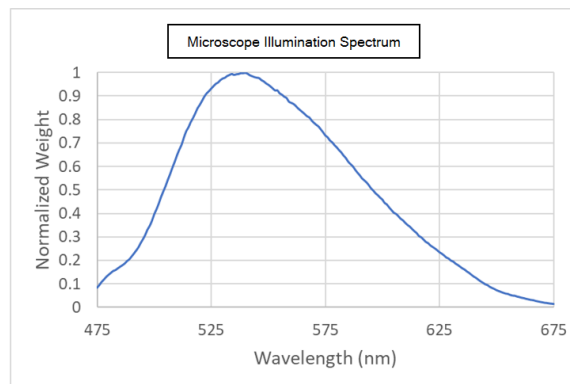
Figure 11: Example Zygo Microscope Illumination Profile

For microscope objectives, the nomenclature is standard regarding the number of design wavelengths. An achromatic objective is optimized at 2 wavelengths, an apochromatic objective is optimized at 3 wavelengths. A super-achromatic objective typically refers to an achromatic objective that is optimized over some additional near ultraviolet or near infrared wavelength range (6).

We will be optimizing over 5 wavelengths; the objective is therefore apochromatic. Further, the wavelengths will be weighted by the relative illumination values seen in Figure 11. The wavelengths used are for the peak illumination and the two wavelengths at 30% of peak intensity. These values have been shown to correlate best with performance across the full bandwidth. As the design progresses to a near final state, additional wavelengths may be

29

added to confirm acceptable performance across the full spectrum. This should wait until near completion to reduce calculations during iterative optimization process.

Table 2: Wavelength table adequate for apochromatic objective design.

		Wavelength (μm)	Weight	Primary
✓	1	0.496	0.300	○
✓	2	0.512	0.700	○
✓	3	0.540	1.000	◉
✓	4	0.582	0.700	○
✓	5	0.617	0.300	○

2.d. Effective Focal Length

The ratio of tube lens Effective Focal Length (EFL) to objective EFL defines the magnification of the objective. Different microscope manufacturers use different tube lens focal lengths; therefore, the actual objective magnification will depend on the microscope on which it is installed. We will be assuming a 200 mm focal length tube lens. Therefore, we require a 1x objective to have a focal length of 200 mm, nominal.

$$m = \frac{EFLTubeLens}{EFLObjective} = \frac{200\ mm}{200\ mm} = 1x$$

The objective is 'infinity corrected' meaning that light emerging from a point on the object emerges collimated from the exit pupil of the objective. This means that, now that we know the EFL, we can perform optical design of the objective without including the profiler in the model. This simplifies our task.

2.e. Parfocal Distance

Another characteristic of the microscope objective that is important to many customer use cases is the parfocal length. This distance is measured from the flange of the objective to the object plane. Therefore, this distance is the sum of the Working distance as defined in the previous section and the distance from the flange to the last mechanical surface. A microscope may commonly be equipped with a turret, onto which several objectives of varying magnifications are installed. This could be done so that several measurements over a varying range of spatial resolutions can be taken in conjunction.

Multiple objectives may also be desirable so that the ease of alignment of one objective may be leveraged before switching to the preferred objective for taking measurements. To illustrate the last point, consider using a visual microscope where a small feature is to be inspected. The operator will often start with a low magnification objective to identify the feature within the larger context of the surface and center the feature within the field before switching to a higher magnification objective.

It is therefore desirable that focus be maintained (as closely as possible) when switching between objectives to minimize the amount of realignment is necessary. Many manufacturers will establish a standard for the parfocal distance. Zygo uses 60 mm for their 'standard' objectives and 120 mm for their LWD (Long Working Distance), SLWD (Super Long Working Distance), and GC (Glass Compensated) objectives.

Figure 12: Turret-Mounted Interference Objectives[iii]

Within Zemax, we've created a dummy surface as a thickness solve (sum of surface thicknesses) from the image plane to another dummy surface that represents the objective shoulder. This is constrained during optimization in the Merit Function by CTVA – Center thickness value = 120 mm.

2.f. Working distance

The Working distance (WD) of the objective is the distance from the last mechanical surface of the objective to the surface under test. The surface under test must be placed at the object plane to be focused onto the detector, located at the image plane. The

[iii] Image from: https://www.zygo.com/products/metrology-systems/3d-optical-profilers/key-features/profiler-objectives

system has finite conjugates in object and image space (when the profiler head is considered) and the only focus adjustment in the system is to physically move the part under test until it coincides with the object plane. Therefore, the working distance of the object cannot be changed, or imaging quality will be degraded. Specifically, after moving more than 1 Depth of Field, the system may no longer be diffraction limited. Further, once aligned, the position of the surface under must satisfy the Zero OPD condition between the reference and test legs. Therefore, the working distance is a function of the optical design and cannot be changed outside of the deviation from manufacturing tolerances.

Working distance is a critical parameter of a microscope objective. A longer WD reduces the risk of damage to the objective while moving the samples or aligning for measurement. The sample may be moved into position within the test area by hand. A motorized vertical stage is used to bring the surface under test into best focus and to find the fringes for measurement. These operations are a high risk to damage to the objective AND the sample from 'crashing' the objective for objectives that have small working distances. For very high magnification objectives with very short working distances, this becomes increasingly important.

There are also applications where the top surface of the sample is not the surface under test. If the surface under test is recessed from the top surface of the sample, the depth of the sample would eat into the available working distance. This second point is a more common concern for the 1x objective that is the topic of this paper. The Working Distance fundamentally limits the depth at which a feature can be measured.

An existing 1x LWD Michelson objective has an 8 mm WD. We will require the new design to allow for 10 mm WD, with a 'stretch goal' of 12 mm. This would be a significant improvement for the customer. This is constrained during optimization in the Merit Function by MNCA – Minimum Center Thickness of Air = 12 mm.

2.g. Numerical Aperture

The Numerical Aperture (NA) of the objective is a function of Entrance Pupil Diameter (EPD) and EFL. Since the EPD is standard across the objective product line, and EFL is

known, this requirement is set at 0.03. This is a critical parameter of an optical system as it defines the optical resolution, which is discussed in i.2.

NA is defined by setting the Aperture Type; we've set Aperture Type to Entrance Pupil Diameter. The NA can be reported within the MFA using operand ISNA since the model is configured with the test surface at the image plane.

2.h. Maximum Field Angle/Field Number

Maximum Field Angle and Field Number (Fn) are given as a single requirement in the table because they linked by the relationship $f = h \tan(\theta)$. Where f, effective focal length, is 200 mm, and h is the object height. Maximum Field Angle is the highest input angle at the entrance pupil of the system that we will design for. So, for a Max Field Angle of 3.6°, we expect the Full Field of View (FFoV) to be ˜25.2 mm. The Field Number is related to the FFoV by the following equation:

$$FFoV = \frac{Fn}{Mo}$$

We're conveniently designing a 1x objective, so Mo = 1 and we get FFoV = 25 = Fn. The difference between 25.2 and 25 is a bit of rounding error in the choosing Field Angle; it doesn't affect the actual FoV as seen in the profiler, which is completely defined by the EFL of the objective.

There is a caveat to nomenclature that is worth mentioning here as it comes up in discussion about appropriate optical performance metrics in the following section. Field Number and Magnification are related to the EFL's of the objective and tube lens. However, Zygo profilers are compatible with interchangeable tube lenses that change the system magnification. These "Field Zoom Lenses" or "Zoom Tubes" range from 0.5x (100 mm equivalent FL) to 2.0x (400 mm equivalent FL).

Imaging	Accessory	Part Number	Description
	Field Zoom Lens	6300-0522-02	0.5X Zoom Lens; standard with Nexview models
		6300-0523-02	0.75X Zoom Lens
		6300-0524-02	1X Zoom Lens; standard with all models
		6300-0525-02	1.5X Zoom Lens
		6300-0526-02	2X Zoom Lens; standard with Nexview models
			Discrete lenses provide high quality and flexible imaging. Lenses purchased separately include a protective case and end caps.

Figure 13: Zygo Optical Accessory Profiler Guide section with available Field Zoom Lenses. (Zygo OMP-0594N 08/22)

33

Throughout the paper, we will continue to refer to "System Zoom" when we are talking about the FoV and spatial sampling of the system with the 1x zoom tube installed.

Magnification	1X	Field of View (mm) based on Zoom and Cam 1600 x 1200 Full FOV 1000 x 1000 Square FOV	0.5X Zoom All Zoom o	Spatial Sampling based on Zoom (μm/pixel)	
Design	Michelson	0.5X	---		
NA	0.03	6300-0522-02	17.49 x 17.49*		
Working Dist (mm)	8.0	0.75X	18.57 x 13.92		
Optical Res (μm)	9.50	6300-0523-02	11.60 x 11.60		
Slope Limit (deg)	1.34	1.0X	13.89 x 10.42	0.5X	17.49
		6300-0524-02	8.68 x 8.68	0.75X	11.60
Parfocal Dist (mm)	122.8	1.5X	9.28 x 6.96	1.0X	8.68
Thread	M25	6300-0525-02	5.80 x 5.80	1.5X	5.80
Turret Mountable	Yes	2.0X	7.00 x 5.25	2.0X	4.37
ZYGO P/N	6300-0318-01	6300-0526-02	4.37 x 4.37		

Figure 14: FoV and Spatial Sampling for an equivalent Zygo 1x LWD Michelson objective. (Zygo SS-0122 08/22)

Based on this, we've chosen to define field points for the Maximum field of 0.5x, 1x, and 2x system zooms, as shown in Figure 16. Field points are set along ± Y field due to asymmetry of the system along that axis but only half of the symmetrical X axis field.
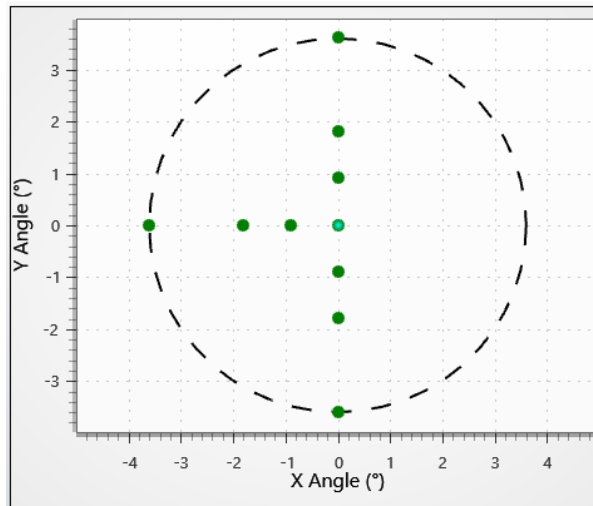
Figure 15: Field Plot from Zemax Field Data Editor for 1x ZWF.

2.i. Diffraction Limited Performance

Because we have some latitude in the definition of diffraction limited performance, we will give an overview of several methods to define optical performance and their diffraction limit. During design, it's often preferred to choose optical performance metrics that have a

low computational cost to reduce design cycle time. Controlling this through the Zemax Optimization Wizard is a great option.

i.1. *Point Spread Function*

An ideal system, a hypothetical construct with no aberrations, will image an ideal point in the object plane to another point in the image plane. The resulting image (called the Point Spread Function or PSF) is that of an Airy disc. It has the appearance of a bullseye and can be mathematically represented as a Bessel Function. The energy that has escaped from the image of the point is due to diffraction through the circular aperture. The resolution of this system, though it is without aberration, is limited by the amount of diffraction exhibited in the airy disc.
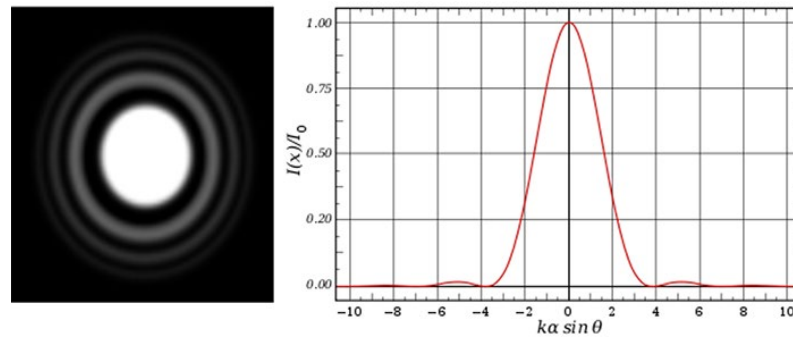
Figure 16: The PSF of a system with a circular aperture in the form of an Airy disc (left) and a linear slice profile of the normalized intensity.

During the optical design process, if the system resolution exceeds the diffraction limit, it will not improve the overall performance of the objective. So, we don't attempt to make an ideal system, but instead we try to reduce aberrations until the system is not appreciably worse than the ideal diffraction limited performance.

i.2. *Optical Resolution*

To reasonably define what qualifies as diffraction limited performance, we will need to determine the resolution of the system. There are several ways to define the system resolution, such as the Rayleigh and Sparrow Criteria:

- Rayleigh Criterion; $Res = \frac{0.61\,\lambda}{NA}$

- Sparrow Criterion; $Res = \frac{0.5\,\lambda}{NA}$

35

Zygo uses the Sparrow Criterion, where center wavelength = 570 nm and NA = 0.03 for the 1x objective. This results in an optical resolution of 9.5 μm. Given the spatial sampling defined in Figure 14, this means that the system only needs to be diffraction limited out to 1x system zoom. The system is pixel-limited beyond that where the spatial sampling is larger than the optical resolution.
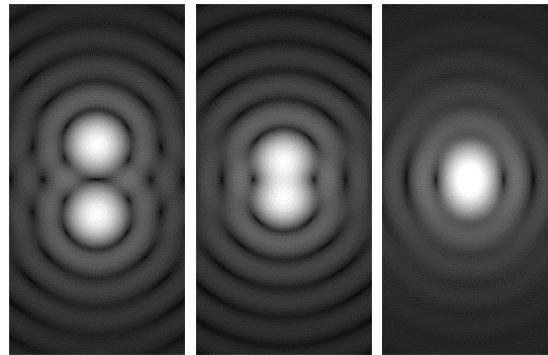
Figure 17: Image of two diffraction-limited points that are easily resolved (left), that are at the limit of resolvability per the Raleigh Criterion (center), and that are at the limit of resolvability per the Sparrow Criterion. [iv]

However, there is no universally agreed requirement that defines a system as diffraction limited. We will go over several of the most common options below and some of their relative merits. Many commercially available objectives don't even explicitly state optical performance requirements within their spec sheet. Instead, just assure the customer (or heavily imply) that the performance is diffraction limited. Similarly, we have some latitude to determine which Optical Performance Metric is best suited for our requirement if the choice is appropriately justified for our workflow.

i.3. *Strehl Ratio*

Through an ideal system, image of an ideal point will result in a diffracted The Strehl Ratio (SR) is the ratio of the peak of the PSF between ideal and predicted as-built system performance. If the SR is > 0.8, then the system is said to be diffraction limited.

[iv] https://www.e-education.psu.edu/mcl-optpro/book/export/html/803
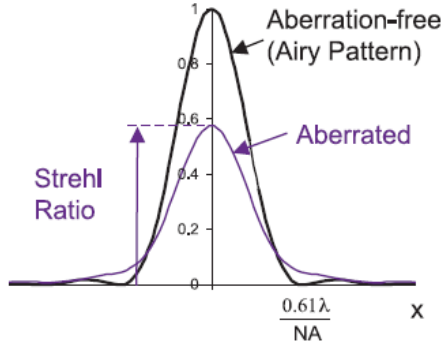
Figure 18: Normalized intensity plot illustrating the Strehl Ratio (5)

i.4.   *Optical Path Difference*

i.4.1.   *Peak-to-Valley*

Peak-to-Valley (PV) gives the OPD between the highest and lowest points in the OPD. The Rayleigh quarter-wave Criterion states that an optical system with $\lambda/4$ PV OPD of power or spherical will have an SR of 0.8. (5) Therefore, this should be an appropriate threshold for diffraction-limited performance.

i.4.2.   *PVr*

Peak-to-Valley is often reasonable to use during the design phase. In practice, during measurement, it is defined by 2 pixels (the highest and lowest), which can often be misleading. This leads to e.g., a wide variation in measured values between metrology systems, depending on their resolutions. (7) The robust Peak-to-Valley (PVr) applies some amount of filtering to improve this issue and system-to-system measurement reproducibility.

This value is defined as the PV of the first 36-term Zernike fit map plus 3 times the RMS of the 36-term Zernike fit residual. Fit residual is everything from the original measured data after the 36-term Zernike map. Data outside of the PVr range is effectively clipped.

PVr also has two defined limitations; it cannot exceed the measured PV value and it cannot be less than six times the RMS of the 36-term Zernike fit residual. It must also be confirmed that the number of clipped data points is limited to measurement noise and does not include real data.

i.4.3.   *Root-Mean-Squared*

Root Mean-Squared (RMS) OPD is like PV in that the OPD is analyzed. However, RMS is more predictive of the actual imaging performance of the system. The most commonly

37

used RMS requirement is the Maréchal Criterion, which states that a SR of 0.8 corresponds to an RMS of 0.71 λ, based on a typical balance of aberrations. This is how we will define our system to be diffraction limited at 1x system zoom.

i.5. *Spot Size*

i.5.1. *RMS Spot Size*

RMS Spot Size gives a good approximation of the spot size that contains most of the energy for the given field points. It's based strictly on traced rays, so does not reflect the limitation of diffraction on spot size. The diffraction limited Airy disc can be overlayed as a comparison.
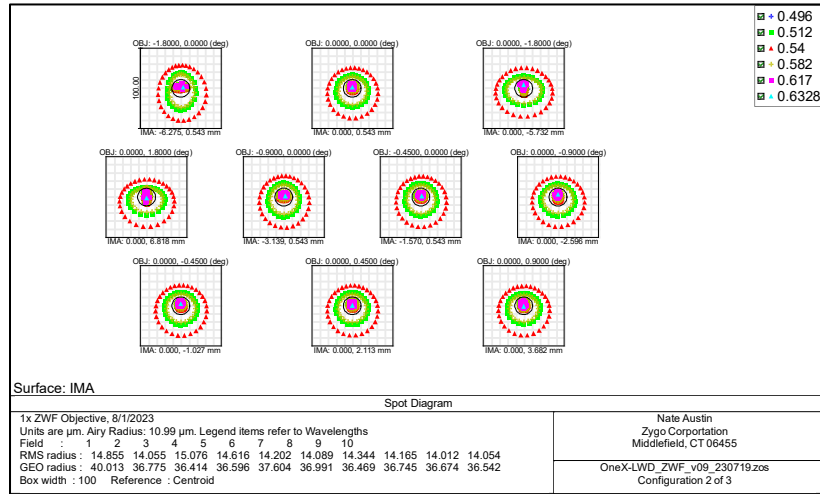
Figure 19: Example of Zemax Spot Diagram, which includes RMS spot radius for each field point plotted.

i.5.1. *Encircled Energy/ Ensquared Energy*

Encircled Energy and Ensquared Energy measure the energy from the PSF contained within a circle of a given radius or a square of a given half-width, respectively, as shown in Figure 20. These results can give a more physical approximation of the spot size because it also considers diffraction. Encircled Energy is convenient because it matches the nominal circular shape of the diffraction-limited Airy disc. Ensquared Energy can be more practical because it quantifies the amount of energy that falls onto the square-shaped pixel of the detector.

38
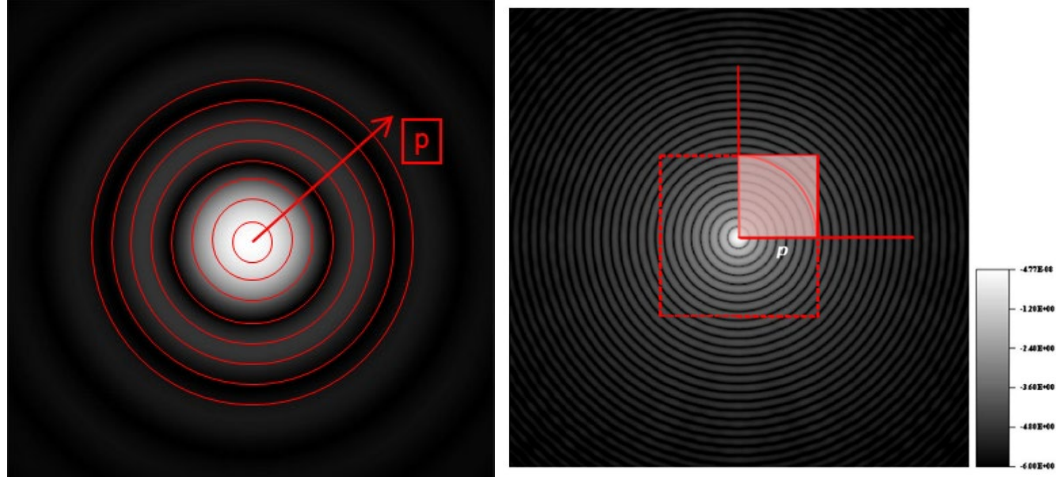
Figure 20: Figure illustrating circles of various sizes (p) centered at the centroid of the PSF. (left). [v] Illustration of ensquared energy from diffraction limited airy disk within square of half-width ρ (right). (8)

i.6. *Contrast*

Contrast in an optical system (distinct characteristic from fringe contrast, which is also a critical feature of interferometric systems and discussed elsewhere in this paper) is a measure of visibility at the detector as a function of the spatial frequency of the input signal. Contrast is a common method to qualify optical system performance. Within Zemax, the Modulation Transfer Function (MTF) reports contrast as a function of spatial frequencies for selected wavelengths and fields.

Two important values limit the spatial frequencies that can be detected by the profiler. The Abbe limit or optical cutoff frequency describes the optical limit based on the resolution of the optical systems, $f_{Abbe} = 2\frac{NA}{\lambda}$, and the Nyquist Frequency, $f_{Ny} = \frac{1}{2p}$, where p is the spatial sampling of the detector. To avoid aliasing, it's recommended to have $f_{Ny} \geq f_{Abbe}$. (9)

MTF has a larger cost in calculation time during the design cycle than e.g., OPD. For this reason, we haven't used it during optimization. Instead, we have designed based on the

---

[v]https://www.optikos.com/articles/encircled-energy-and-ensquared-energy-on-lenscheck-lens-measurement-systems/

39

Maréchal criterion mentioned above, and we will use MTF as a validation test requirement. This is discussed further in section 8.
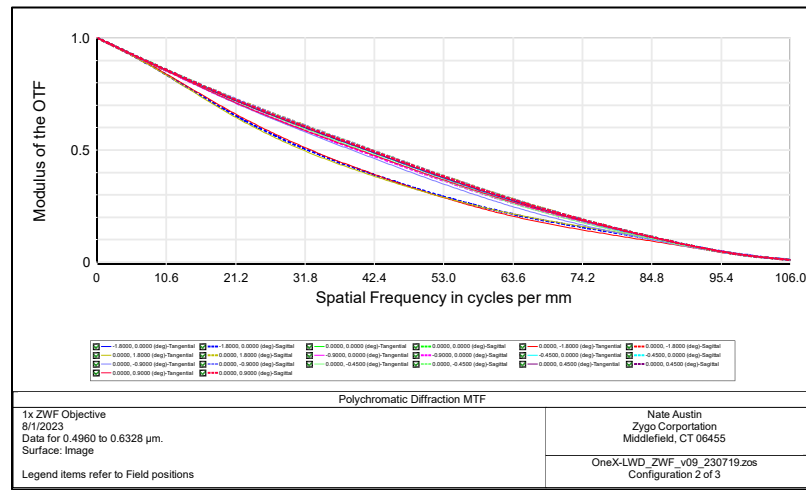
Figure 21: Example of Zemax MTF plot as a function of spatial frequency for various field points.

2.j. Distortion

Distortion is defined as a change in magnification as a function of field. The most obvious impact on an optical system is the tendency to distort straight lines into curved ones. A convenient way to see the effect is the image of a rectangular grid. The direction of the change determines how the distorted image appears. Negative distortion, called pincushion distortion, decreases magnification as a function of image height and looks more rounded than the original grid. Positive distortion, called barrel distortion, increases magnification as a function of image height and looks pointier.

A goal of 0.1% on a detector with and 800-pixel HFoV will have < 1 pixel of distortion. This parameter is constrained in Zemax MFE by DIMX = 0.1.
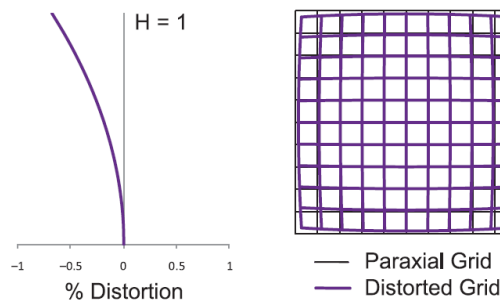
Figure 22: Figure showing an example %Distortion plot with a negative distortion (left) and the resulting pincushion distortion of a grid from (right). (5)

2.k. Lateral Color

Lateral Color is a change in magnification as a function of wavelength. This is worse than distortion since images of different sized (depending on wavelength) will have different sizes and cause a blur to the image. This is important to specify independent of optical performance because e.g., OPD is evaluated for each ray bundle and referenced to the chief ray or centroid. That is, two wavelengths may be individually diffraction limited, but not overlap to form an acceptable image.

For our purposes, we'll define Lateral Color the same way that Zemax does, as the difference between chief ray intercepts for the 2 extreme wavelengths defined. Lateral Color can be constrained with the LACL operand.
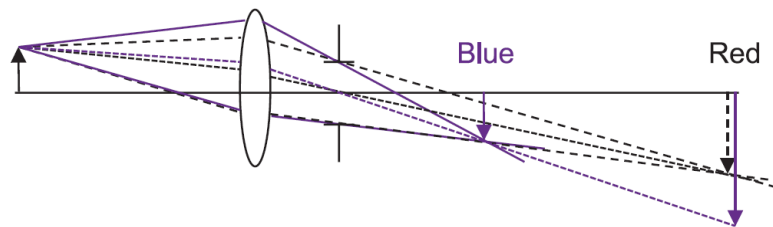
Figure 23: Lateral Color results in a change in Magnification as a function of wavelength. (5)

2.l. Axial Color and Field Curvature

These aberrations are worth mentioning as a contrast to distortion and lateral color, above. They are important to understand within the optical design process, but they do not have a formal system requirement. Axial color is a change in focus position with a change in wavelength and field curvature is a change in focus position as a function of field position (squared).

The change in focus manifests as degradation of the imaging quality of the objective, so these aberrations are included in the requirement for optical performance and constrained simultaneously. They must necessarily be constrained very well to meet that requirement, though they can be among the largest error contributors.

41
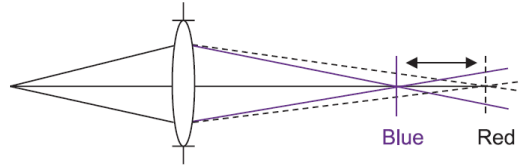
Figure 24: Axial color is a change in focus as a function of wavelength. (5)
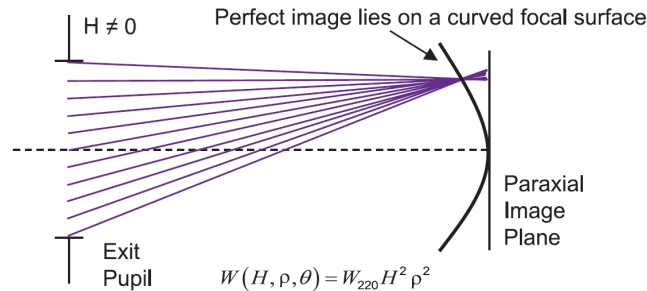
Figure 25: Field Curvature is a change in focus as a function of field. (5)

2.m. Telecentricity

Microscope objectives are generally object space telecentric. This means that all chief rays through the center of the aperture stop will emerge from the system parallel to optical axis. In this configuration, there is no change in image size with object distance. The focus in a microscope is generally set by adjusting the distance from the objective to the object so that the object falls within the object plane. Unlike some other optical systems, there are no internal adjustments to set the focus. Telecentricity will decouple magnification from focus.

Coherence scanning objectives also move to modulate the fringe envelope across the surface of the part under test or to find test surfaces with different heights. Without image space telecentricity the image size would change during the scan, which is obviously unacceptable for critical inspection equipment.

To achieve object space telecentricity, the aperture stop must be located at the front focal plane of the objective. That is, light that is collimated in object space will focus to a point at the aperture stop.

42
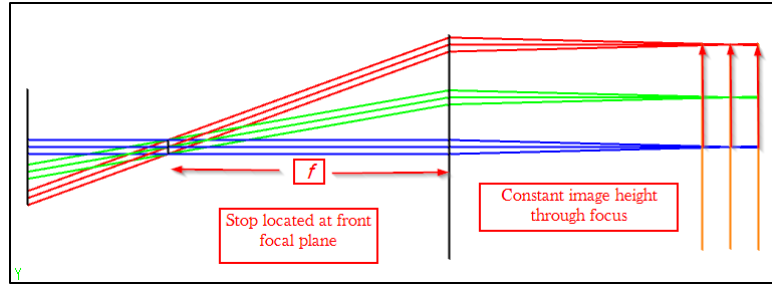
Figure 26: Image height in telecentric system is independent of focus position.
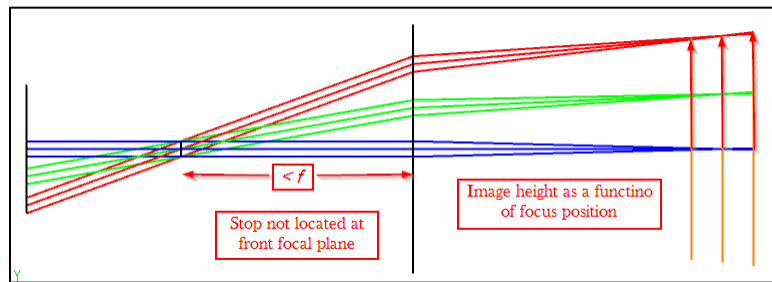
Figure 27: Image height in non-telecentric system changes as a function of focus position.

2.n. Temperature Range

n.1. Operating Temperature

The operating temperature requirement is a temperature range over which the system is expected to operate and continue to meet all other functional requirements. For this objective, we expect it to be used over the same operating temperatures as the optical profilers. The specified range was found in Zygo Spec Sheet SS-0121 for NexView NX2 profiler product, which is a typical range for all Zygo optical profilers.

Glass and metal have dissimilar Coefficients of Thermal Expansion (CTE), so they will expand at differing rates with a change in temperature from the nominal lab temperature at which they were assembled. First, the stress from the thermal expansion/contraction causes strain in the optics, which can be problematic for the most sensitive optics. This is discussed in section 7.e.2. Additionally, expansion of the metal housings will cause changes to air-spaces thicknesses, which potentially results in a change of focus or OPD. Determining this impact is an important part of Optomechanical design but is not discussed in this paper.

n.2. *Shipping Temperature*

The shipping temperature requirement is a temperature range over which the system is expected to be subject to during shipment. The system does not need to meet function requirements over this range. The system needs to survive exposure to the full temperature range without changing performance when returned to operating temperatures. The Shipping Temperature Cycle that the objective will be exposed to, per MIL-STD-810G, is shown in Figure 28.
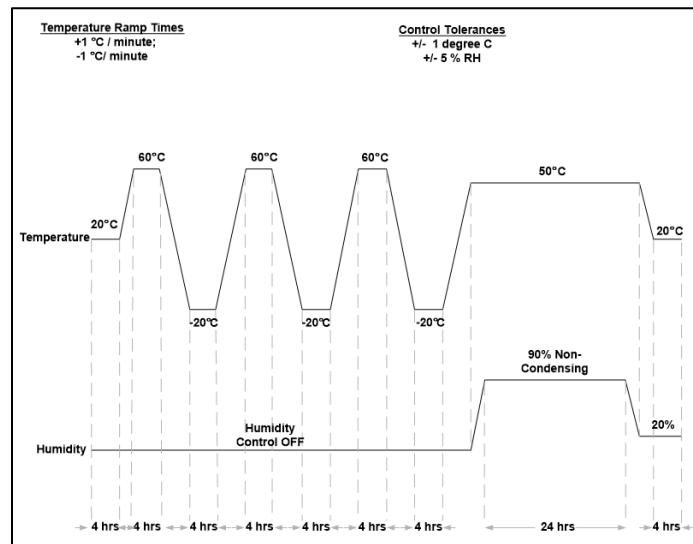
Figure 28: Example Shipping Temperature Cycle an assembly is subject to during validation testing.

The shipping temperature requirement will determine the necessary gap between lens and cell to avoid excessive hoop stress on the optics as well as possible mounting configurations and torque specs to avoid loss of preload.

2.o. *Test Sample Reflectively*

The contrast of fringes within an interferometer are dependent on the relative intensity of the reference and test beams which are interfering. It is relative because the fringe contrast is not a function of absolute intensity, to first order. If the beams have equal intensity, then the interference pattern will have theoretically perfect fringe contrast. As the difference between the test and reference intensity increases, the fringe contrast decreases. So, we must define a sample with optimum reflectivity to determine the appropriate reference and beamsplitter surface reflectances. We've chosen a surface that will be optimized for fused silica. This is discussed further in section 7.a.

44

The absolute intensity does have some secondary impact on the contrast that is worth mentioning. A DC component to the fringe pattern caused by any background light falling on the detector (either from the environment or from scatter within the instrument) increases the floor of the dark fringe and thus reduces the overall fringe contrast.

2.p. Ghost Reflections

Ghost reflections are unintended, reflections from optical surfaces within the system that impact system performance. Due to the auto-illumination configuration within the interference objective, ghosts appear as a bright area at the center of the detector, referred to as the 'hot spot'.

Typical methods to reduce ghost reflections include improved Broad-band Anti-reflection (BBAR) coatings and considerations during optical design. (10) Using a hood is typical for ghost reflection in photographic applications but doesn't help in microscopic objective applications. Based on similar Zygo objective designs and component procurement, we can safely assume that the BBAR coatings cannot be meaningfully improved without significant cost increases. The constraints on design are too restrictive to allow for a feasible design.

We know that, within the optical profiler, the illumination leg is reflected from a Polarizing Beam-Splitter (PBS) before a Quarter-Wave Plate (QWP). This means that the light is circularly polarized at the entrance pupil of the objective and that light that polarized parallel to the illumination at the PBS will be rejected by the PBS toward the source. We can use this knowledge to eliminate ghost reflections using QWP's. Any light that reflects after a QWP at the entrance of the objective will experience a total of 1 wave of retardance: 2x profiler QWP + 2x objective QWP 1. Then a second objective QWP is placed after the lens groups so that the test and reference legs will experience an additional ½ wave for a total of 1.5 waves of retardance and, therefore, transmit through the PBS toward the detector.

A zero-order QWP should be used to mitigate the dependency of retardance.
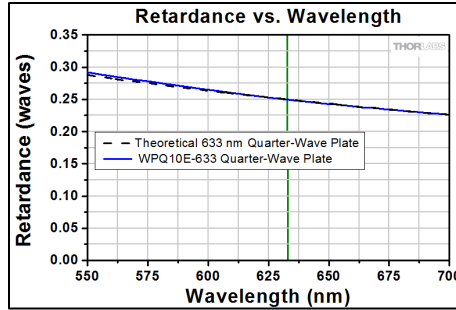
Figure 29: Wavelength dependency for zero-order QWP. [vi]

3. Optical Design

3.a. Design Form Discussion

Because the purpose of a microscope is generally to enlarge the image of the subject, the unit-magnification objective is not well studied. The most challenging objectives are usually those with the highest magnifications and highest numerical apertures.

We desire the objective to provide unit magnification, which is uncommon because it doesn't generally require a microscope for imaging; a much simpler imaging system can provide the same magnification. That is, a less expensive solution would provide comparable imaging resolution of the object if only imaging was required. Interference objectives provide the additional benefit of providing sub-nanometer, areal topographical measurement of a surface. It is beneficial for a manufacturer to have a wide range of available magnifications available. For example, Zygo offers interference objectives from 0.5x – 100x magnification.

[vi] https://www.thorlabs.com/newgrouppage9.cfm?objectgroup_id=8635
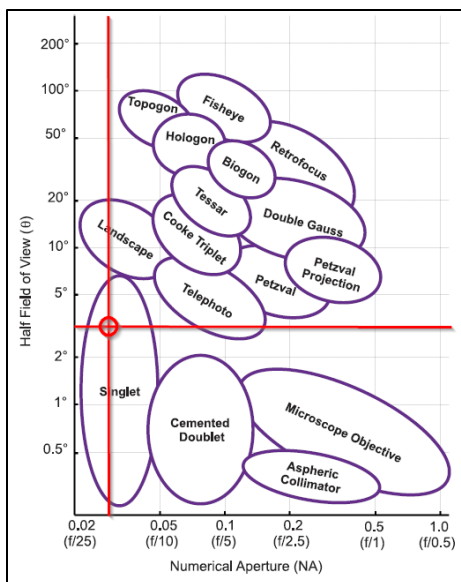
Figure 30: Design Form map showing where the 1x objective would fall if NA and FoV were the only considerations. (5)

A first look at a classic optical design form table shows that we might be able to design a system of similar etendue very simply, but that doesn't include some of the other restrictions that we have. Because the EFL is longer than the parfocal distance, we know this is a telephoto lens, requiring a PN (positive-negative) configuration. But we need another positive lens to bend the diverging chief rays to be parallel to the optical axis. This leaves us with a PNP configuration. This is typical form for low magnification objectives.

3.b. Starting Point

There are multiple approaches to begin the design phase once system requirements and design form are determined. This section contains a few common methods for finding a starting point.

b.1. First Order Design

Here 'first-order' means that the design space is narrowed enough that governing formula are approximately linear. For optical design, this happens with angles in a very narrow range around the optical axis. This is referred to as the paraxial regime, for this reason.

Using the knowledge of our design form from 3.a, we begin a Zemax lens file with Paraxial surfaces vaguely matching our design form. We then add first order properties like

Effective focal length and telecentricity to the MF before solving for a viable first-order design.
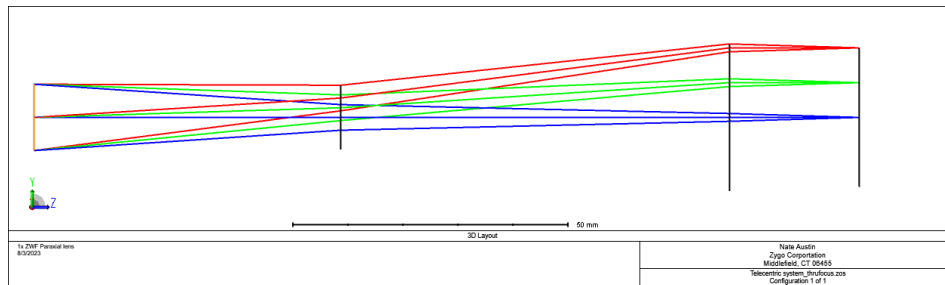
Figure 31: Optical Layout of paraxial design with first order characteristics of 1x objective.

This first-order model can now be fleshed out to a third-order thin-lens model by adding curvature to the surfaces and materials. It would then be further fleshed out into a third-order thick lens model by adding thicknesses to the material. This first order design has 3 lenses, but our final design has 8. This means that this starting point would have a significant amount of design cycles compared to other starting points mentioned below.

b.2.   *Starting from an Existing Design*

A common practice is to start with an existing design within a similar design space and modify it to meet the specific requirements of the new design. In a corporate setting, there may be similar existing products that could be used as a starting point. In our case, there are 2 designs that are worth investigating; a 1x LWD Michelson and a 0.5x ZWF.

b.2.1. *1x LWD Michelson*

The 1x LWD Michelson objective already has EFL and several other system parameters in common. This is a natural choice for a starting point. The heavy NPBS is removed and replaced with the ZWF plates and it's ready for optimization.
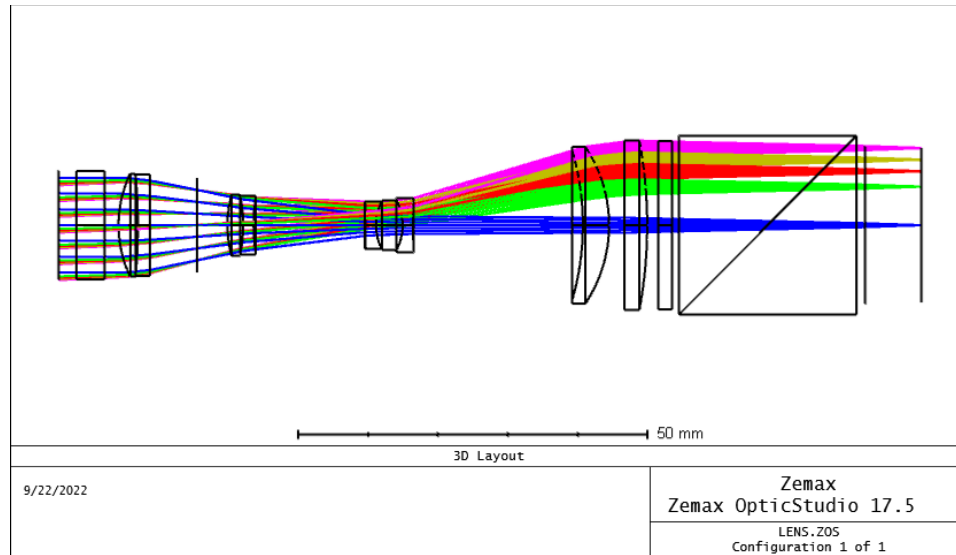
Figure 32: Zygo 1x LWD Michelson Objective.

b.2.2. *0.5x ZWF*

The 0.5x ZWF objective has an effective focal length (EFL) of 400 mm, or 2x the focal length of the 1x ZWF we wish to design. We can therefore take the 0.5x ZWF objective optical model and scale it by ½ to yield an objective design that has a 200 mm EFL. When this happens, the entrance pupil is also scaled. When the entrance pupil is increased to meet the NA requirements, additional aberrations are imparted that need to be corrected through further optimization.
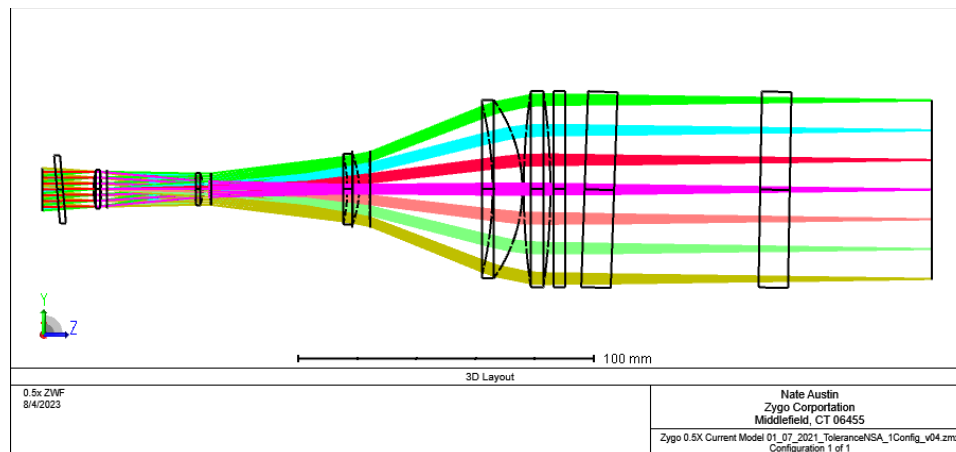
Figure 33: Zygo 0.5x ZWF Optical Layout

b.3. *Automated Lens Design*

This topic is outside the scope of this paper, but it is worth discussing here due to the considerable attention that Artificial Intelligence has garnered in the media with the release of several Large Language Model programs. There is existing research on the use of machine learning within the context of optical design to improve the output of an individual optical designer as well as the quality of the output designs. This type of program may use the existing Zemax API to communicate with Zemax for the actual raytracing analysis.
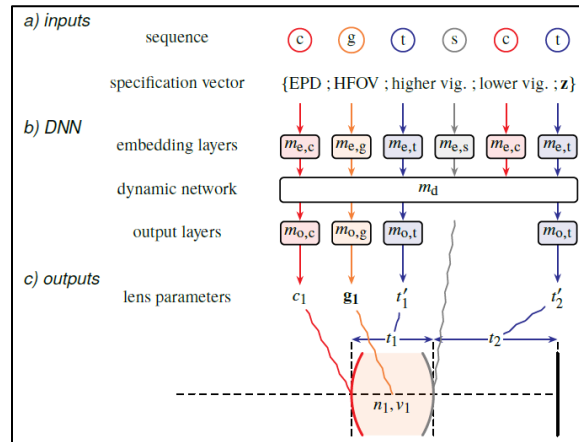
Figure 34: Example workflow of Deep Neural Network framework for automated lens design program. (11)
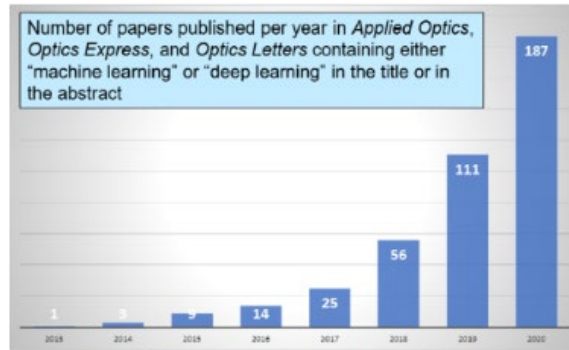
Figure 35: Figure demonstrating the exponential growth of research into automated lens design in recent years. (12)

The prevailing thought is that any "AI" tool would only be useful to provide reasonable starting points for design and require a human optical designer to finalize the design. This is an outline of a basic machine-learning automated lens design program.

- Human designer defines the system requirements.

50

- Human designer develops appropriate merit function to meet those requirements.
- Human runs automated lens design program.
- Automated lens design program returns one or many lens files that can be used as starting point for additional refinement.
- Human designer chooses favorable designs as starting point for further optimization, tolerancing, etc.

This type of analysis can quickly return several viable lens files that meet system requirements but have a variety of design forms. Or this method can quickly converge on the optimal design form. Or possibly, an unexpected design form is identified in an unexplored design space.
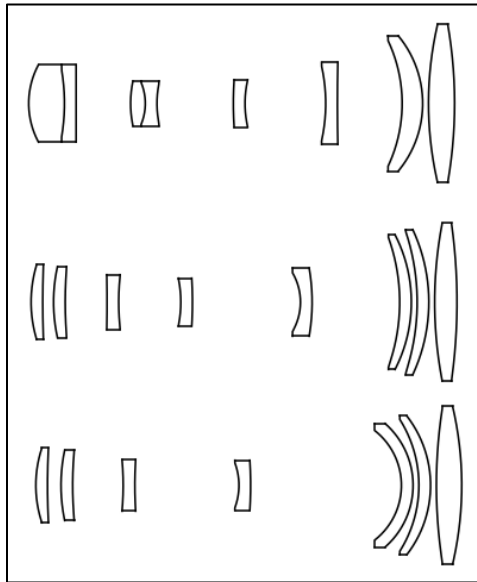
Figure 36: A series of design forms generated by an automatic lens design program.
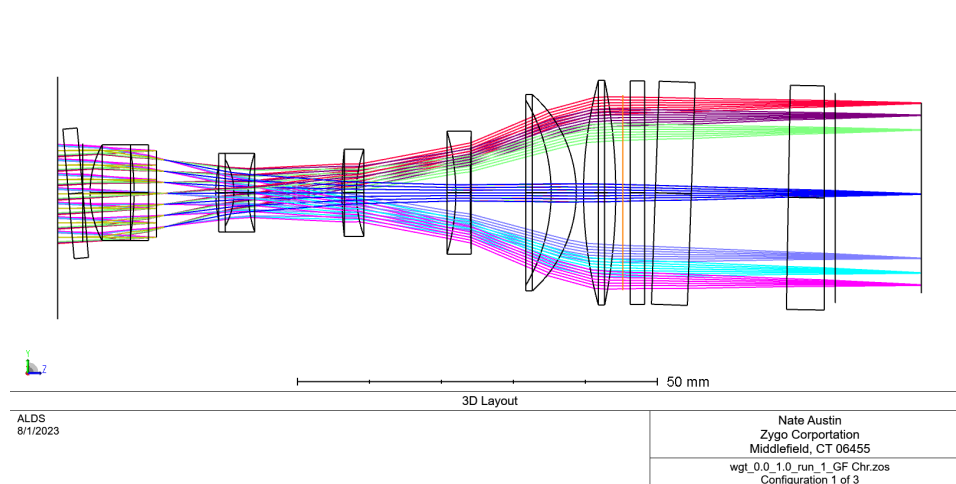
Figure 37: Design forms from automated lens design program with additional optimization by optical designer.

3.c. 1x ZWF Starting Point

For the 1x ZWF starting point, we attempted all 3 approaches to offer a variety of options. In this case, starting with the 0.5x ZWF converged quickest on an acceptable nominal design. A discussion on Optimization can be found in APPENDIX A. Optimization Operands that were use can be found in APPENDIX B.

4. Nominal Design

After Optimization, we were able to achieve a nominal design that meets our design requirements. The design has a nominal EFL of 200 mm, nominal parfocal distance of 120 mm, and nominal WD of 12 mm. It is also telecentric in object space.

4.a. Optical Layout
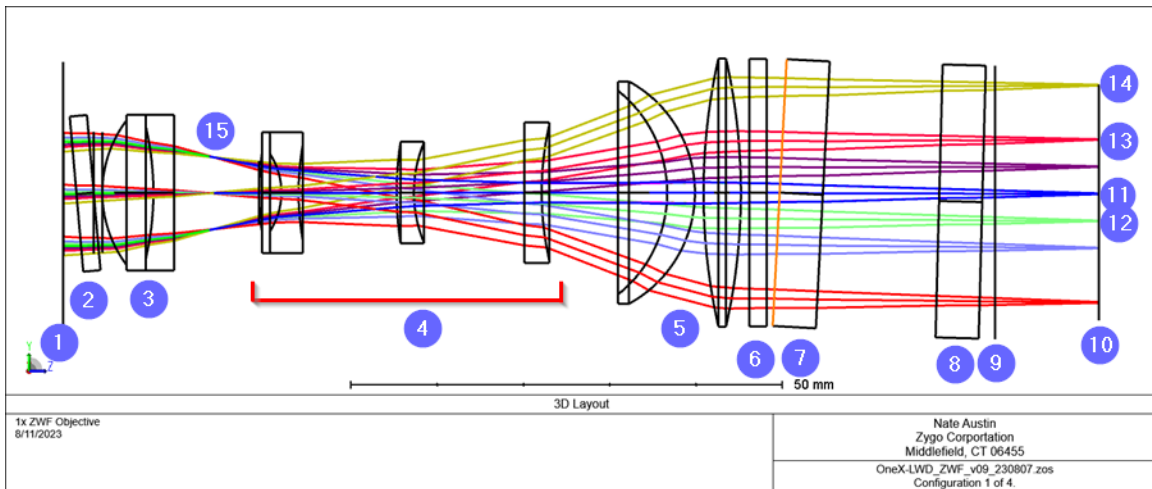
Figure 38: Optical Layout of 1x ZWF Objective at 0.5x System Zoom

All the major points of interest are enumerated in Figure 38:

1. Objective shoulder – interfaces with optical profiler
2. QWP 1 – In conjunction with QWP 2, eliminates ghost reflections from interlaying surfaces.
3. Positive Group
4. Negative Group
5. Positive Group
6. QWP 2 - In conjunction with QWP 2, eliminates ghost reflections from interlaying surfaces.
7. Reference plate – Reference surface is the left side of the plate as shown.
8. Beamsplitter plate – Beamsplitter surface is the left side of the plate as shown.
9. Objective cover – Last mechanical surface of the objective, working distance is measured from this location.
10. Image plane
11. On-axis ray bundle
12. Full Field of View – 2x zoom tube.
13. Full Field of View – 1x zoom tube.
14. Full Field of View – 0.5x zoom tube.
15. Aperture stop – located to create telecentric object space for the objective.

53

4.b. OPD

Our design parameters did not include a PV OPD requirement, but this is a very good way to visualize what is driving the optical performance. From the separation of the colors, we can see the system has some chromatic aberration. There is also 5th order spherical aberration. The high slope of the OPD at the edge of the pupil suggests that the design may be sensitive to alignment.
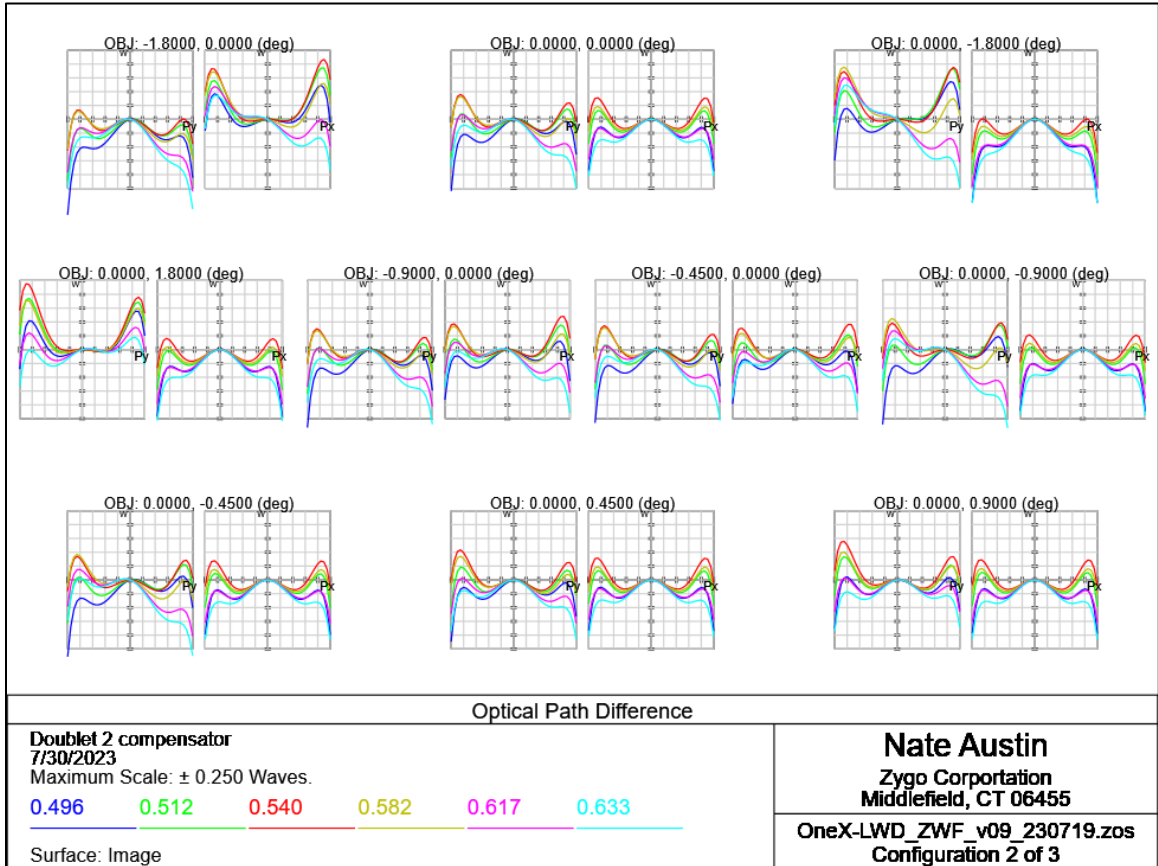
Figure 39: OPD plot for various fields out to 1x system magnification

4.c. RMS WFE vs Field Angle

The RMS WFE vs Field Angle plot gives us a more direct measure of nominal performance. This graph can overlay the diffraction limit, ~0.071 Wv RMS. In the 3 graphs in Figure 40 and Figure 41, the wavefront is diffraction limited across the field for 1x system zoom.
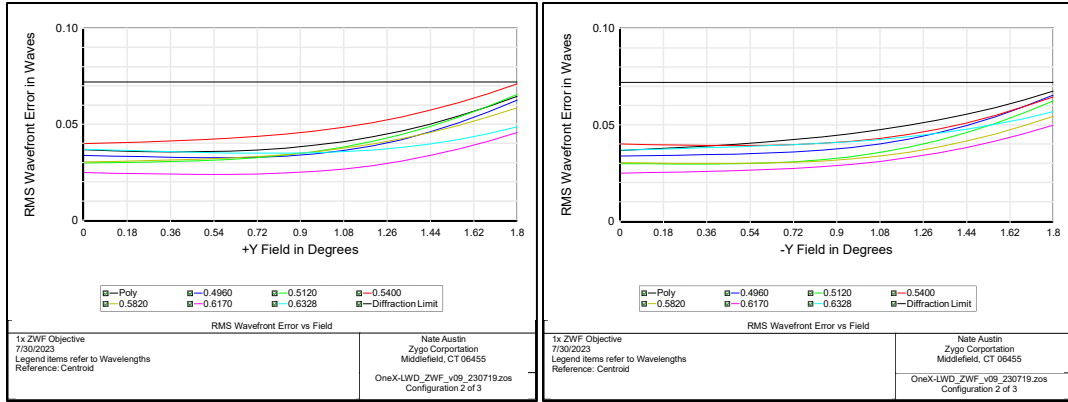
Figure 40: Nominal RMS WFE along +/- Y field at 1x system magnification
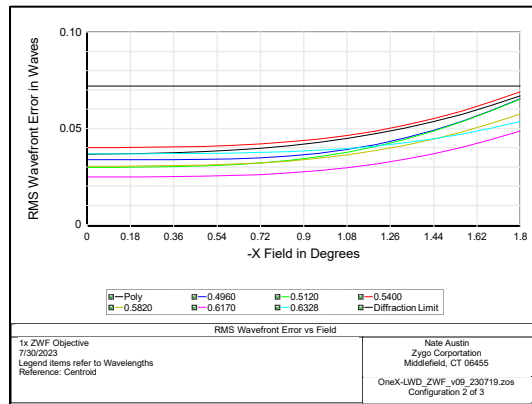
Figure 41: Nominal RMS WFE along + X field at 1x system magnification. The system is symmetrical about this axis.

4.d. Distortion
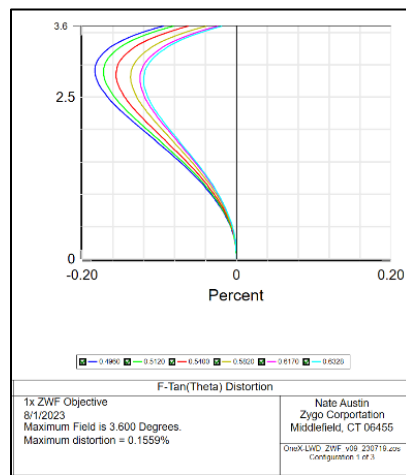
Figure 42: F-Tan Theta Distortion

4.e. Lateral Color

Lateral Color is given as 0.25 pixel. This translates to 2.2 µm out to the 1x system zoom field angle of 1.8° and 4.4 µm out to the 0.5x system zoom field angle of 3.6°. Lateral requirements are met for both fields.
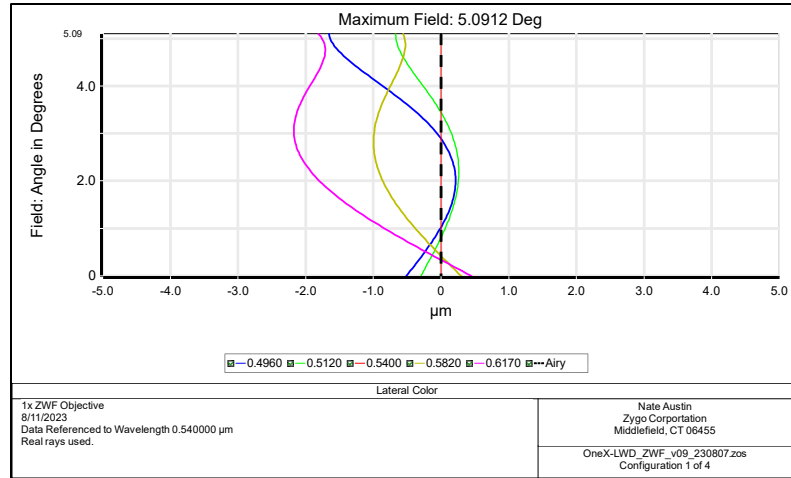
Figure 43: Lateral Color remains under 2 µm across the field.

5. Tolerance Analysis

5.a. Tolerancing Background

During the nominal optical design process, the optical system is presumed to have ideal surfaces located at the exact position described in the Lens Data table. For a commercial application, the customer is not expected to care about the quality of the nominal optical system; they would instead care about the quality of the physical system that they receive. Therefore, the most important design consideration is the 'as-built' performance. This is the expected performance for any individual physical sample of the designed system.

Each system built will have slightly different errors associated with the lens surface figure and positions. Lens surfaces are not perfectly spherical, the center of curvatures for each surface will not perfectly coincide with the optical axis of the system, and the air spaces will not be maintained to sub-micron precision. So, the practice of tolerancing a system is to assume that none of the specified features within the system are perfect and to instead bound the amount of error that is tolerable such that an acceptable system is ensured during assembly i.e., as-build performance.

56

Because each system is expected to have a unique, quasi-random set of errors for all components and features, the impact to the as-built performance of an individual sample of the system cannot be reliably predicted. Therefore, the most common and reliable method of performing tolerance analysis of an optical system is to use Monte Carlo analysis. This method applies a random amount of perturbation to each defined feature within an allowed tolerance band and evaluates the resulting impact on the system performance metric. This process is repeated as many times as necessary to develop a statistically significant data set; hundreds to thousands of iterations are common.

An initial set of tolerance values are chosen and analyzed before refining the estimates based on the predicted yield, or percentage of systems that are expected to have adequate performance. Having reasonably close initial values for tolerances can therefore help to reduce the number of iterations required to converge on final toleranced design. The initial tolerances can be chosen a few ways:

- Use of "Commercial Grade" tolerances; these tolerances are considered 'easy' for a manufacturer to achieve without any additional tools or time. Selecting looser tolerances may not reduce the cost of the system, so these can often be considered the loosest tolerances considered.

- Experience with the design form; the design may be based on similar, fully toleranced designs. The new design may be expected to have final tolerances in a similar range.

- Knowledge of the intended assembly method; different assembly methods will have different tolerances associated with them. Using tolerances generally achievable on the intended assembly method is a good place to start. This is discussed further in section 6.a

After a Monte Carlo run, the tolerances should be adjusted depending on the as-build yield:

- If the yield does not meet the requirement, then the highest-sensitivity tolerances should be evaluated and tightened, if possible.

- If the yield exceeds the requirement, then the lower sensitivity tolerances can be loosened to the commercial limit to improve the manufacturing cost.

It is therefore possible for the intended alignment method to change, based on the sensitivity of the mechanical alignments required to meet system performance requirements.

5.b. Tolerance Operands

Like the Optimization Operands within the Merit Function Editor, during design optimization, it is imperative to understand the function of each Tolerance Operand within the Tolerance Data Editor. may be multiple The Tolerance Operands chosen should represent the actual mechanical and optical tolerances of the system. Therefore, the tolerance operands should reflect the assembly methods chosen and the constraints and alignments they necessitate.

There is no single correct way to build a tolerance model. There is often more than one way to tolerance a single constraint. Just as the Merit Function will evolve over the course of the design phase, Tolerance Operands will be updated as an understanding of the system sensitivities develops.

b.1. *TEDR – Tolerance on element radial decenter in lens units*

Next consider a lens with a concave surface that has a flat bevel which contacts a flat mechanical surface or the simpler case of a plano surface. The interface between the flat bevel and the lens seat is a plane and they may slide with respect to each other. The optical axis of the lens will move the same amount. This situation requires true radial decenter tolerance, TEDR.
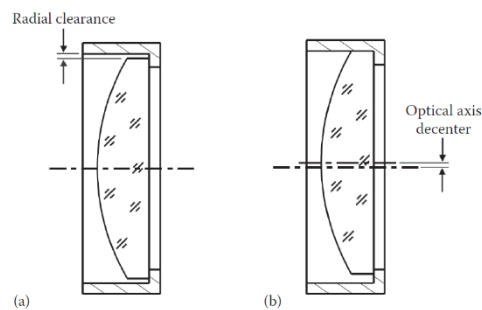
Figure 44: Example of mounting scheme where optics has true radial runout tolerance.

Handbook of optomechanical Engineering; chapter 7

58

b.2. *TETX/TETY – Tolerance on element tilt about X/Y in degrees*

When each lens is assembled to within its manufacturing tolerances, there will still be some non-zero error in that position, regardless of how the lens is aligned. One of these errors is radial decenter, measured as the distance between the center of curvature of the first surface in the system to the optical axis of the system. This could be caused because the lens is not centered within the housing or the housing is not coaxial to the optical axis of the system or, more likely, both. Another error is the tilt of the lens relative to the optical axis. This angle can be thought of as the angle of the first surface normal relative to the optical axis of the system prior to any radial decenter.

The mounting of the lens should be considered when choosing between these tolerances, and there very well may be both. Here are two common situations:

Consider a convex surface that seats with the optical surface against a circular edge. The edge that defines the first surface position will have a mechanical tolerance on concentricity that is applied as a radial runout. However, the lens will not move side to side since that spherical surface is constrained. The lens surface will not change, and the lens will instead roll around on that mechanical edge. This situation should be toleranced as an element tilt about the center of curvature of that surface. A coordinate break, with thickness set to the surface's radius of curvature and tolerances with TETX/TETY is required.
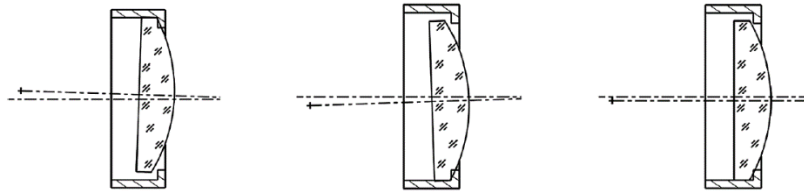
Figure 45: Default lens alignment tolerances create unrealistic models. (13)
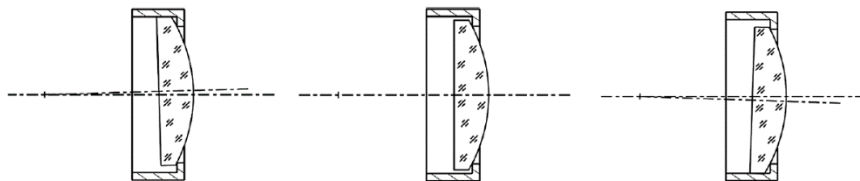
Figure 46: A realistic tolerancing model accurately describes reality. Here radial clearance error causes the lens to roll in the cell resulting in a tilt about the center of curvature. (13)

59

b.3. *TSTX/TSTY – Tolerance on Standard surface tilt X/Y in degrees*

In addition to the element tilts and decenters, it's useful to tolerance individual surfaces for tilt. This can be used to assign e.g., a wedge tolerance to an optical element. When tolerancing an individual surface, a tilt and a decenter will result in identical alignment errors.

In early tolerance schemes, all surfaces might be toleranced individually to better understand the sensitivities within the system and develop the necessary assembly/alignment methods before moving on to a more robust scheme that tolerances them as practical elements. Here, we're using a combination of TEDR, TETX/TETY, TSTX/TSTY to tolerance our element and surface location errors, but there are other sets of operands that will work. It is most important that the chosen tolerance operands accurately reflect the systems practical physical constraints.

b.4. *TIRR – Tolerance on Standard surface irregularity*

One important feature of an optical system is the quality of the surfaces that make up the system; the surface-to-air interface is the portion of the system that contributes all the optical power, after all. The error is described as the deviation of the surface from a perfect sphere, for spherical surfaces, or from a perfect plane, for plano optics. More generally, it could be described as the deviation from the prescribed surface shape, but, for simplicity, let's limit our discussion to the specific cases of spheres and planes. Most optical surfaces in commercial optical systems will take one of these two forms.

Zemax includes a default operand for tolerancing surface irregularity, TIRR. During each Monte Carlo run, a single value will be assigned as the TIRR perturbation within the given tolerance band. However, describing the error of a 2-D surface using a single-value perturbation is problematic. The surface cannot be completely described, and some reasonable assumptions about the surface must be made to achieve reasonable results.

"The assumption OpticStudio makes when using TIRR is that the irregularity is half spherical aberration, and half astigmatism". The equation takes the following form.

$$\Delta Z = \frac{\lambda_t}{2} \left(\frac{W}{2} \rho^4 + \frac{W}{2} \rho_y'^2 \right)$$

This can be confirmed by applying a given amount of perturbation to a Standard surface type and analyzing the resulting wavefront. We believe there is an issue with this assumed

surface shape. It is well known that the Seidel form of spherical aberration can be partially corrected for by inducing some amount of the Seidel form of power (ρ^2). When a spherical optical surface is measured on e.g., an interferometer to confirm conformance to the surface requirement, any measured power is assumed to be due to the alignment with respect to the instrument and may be subtracted out. The amount of power in the measurement can be arbitrarily induced by setting the distance from the test wavefront center of curvature. The power term is the form of the radius of curvature in the surface, which should be specified separately from surface irregularity. The radius of curvature changes the optical power of the element, but in many systems can be 'focused out' by adjusting e.g., the position of the detector plane. This results in the Zernike form of spherical aberration.

$$6\rho^4 - 6\rho^2 + 1$$

When a plano surface is measured, the power term does result in a true deviation from the ideal shape of the surface. That is, it cannot be aligned out during measurement. However, it usually has the same impact at the system level as power radius of curvature on a spherical surface by adjusting the position of the focal plane. Due to this, it is often useful to specify the power of the surface separately from the irregularity of the surface. In that case the given definition of the TIRR operand is also problematic.

Due to the subtraction of power from the measurement, the Zemax TIRR operand will vastly underestimate the impact of a given surface irregularity on system performance when a focus compensator is used. There are several ways to address this shortfall.

One could simply scale the TIRR operand to give the desired amount of irregularity after subtracting power. However, this will leave an amount of power on the surface that is not being captured during tolerancing. It also doesn't really have a contribution that is ½ Spherical and ½ Astigmatism as stated in the assumptions of the TIRR operand.

A second method is to create a surface where Astigmatism and Spherical can both be specified. Zemax has a surface type called Irregular, which takes the following form:

$$z = \frac{cr^2}{1+\sqrt{1-(1+k)c^2r^2}} + Z_s\rho^4 + Z_a\rho'^2_y + Z_c\rho^2\rho'_y$$

where $\rho_x = \frac{x}{r_{max}}, \ \rho_y = \frac{y}{r_{max}}, \ \rho = \sqrt{\rho_x^2 + \rho_y^2}, \ \rho'_y = \rho_y\cos\theta - \rho_x\sin\theta$.

61

Using this surface type, we can apply tolerances to Zs and Za individually (see TPAR below) such that they are balanced, and their contributions add up to the total intended wavefront error. The angle of the Astigmatism term must also be toleranced separately to allow for a random astigmatism angle on each surface. This means that each surface would require 3 separate tolerance operands instead of one. For this reason, it may be desirable to start by using the first option (scaling the TIRR operand) until it is determined that the system is highly sensitive to irregularity and a more realistic approach is required.

b.5. *TPAR – Tolerance on Surface Parameter*

Each surface in Zemax, depending on the type or surface type chosen, has a series of parameters that can be defined and, more importantly, toleranced individually. This makes the ability to tolerance and individual surface parameter an incredibly versatile tool during the tolerancing process. As mentioned above, we can use this tolerance to individually tolerance several parameters of an Irregular Surface type to create a custom irregularity tolerance.

It's worth noting that, within Zemax, a Standard surface doesn't use any Parameters; they all say "(unused)". When a tolerance for element tilt, surface tilt, or element decenter (among others) is defined, Zemax adds a coordinate break around the surface/element in each Monte Carlo run. The MC simulation then perturbs the corresponding parameter for tilt/decenter on the coordinate break. It is truly fundamental to the tolerancing process.

b.6. *COMP/CPAR – Standard Compensator and Surface Parameter as Compensator*

Another step fundamental to the tolerancing process is defining the compensator. Once all perturbations are chosen randomly for a given Monte Carlo run, the system may be compensated. Effectively, one surface parameter is set to variable, and the system is optimized.

This compensator is generally an airspace being adjusted. There are two common choices for focus compensator. If the position of the detector can be adjusted to coincide with the focus of the system, then the final airspace may be used as the compensator. If the detector position is fixed, some other air space may be used as the compensator. Consider a commercial camera lens, where the flange to detector distance is defined by the camera

mount standard. The focus ring adjusts another lens group internal to the lens to move the image to the detector plane. In that case, the focus must be set by the user so that a range of object distances can be accommodated, depending on the subject being photographed. In both those cases, the thickness of a surface is the compensator, which is included in the COMP operand.

In the 1x ZWF objective, we wish to maintain a constant parfocal distance. Instead of allowing the focal plane to shift, we will allow an element that is sensitive to

When the lens positional tolerances on tilt/runout are small enough that an active alignment step is required, then the tilt/runout acts as a compensator during the tolerancing phase. The tilt/runout is toleranced as a parameter of an appropriate coordinate break using the CPAR operand. We found this necessary during the tolerancing of the 1x system, which is discussed in the next section.

5.c. Sensitivity Analysis

The sensitivity analysis portion of a tolerancing run is critical feedback to improve the manufacturability of the design. The results of the sensitivity analysis, in conjunction with the as-built performance of the system will advise the optical designer of individual tolerances that are too loose (have a very high sensitivity) and must be tightened to achieve system requirements. It can also identify tolerances that are too tight (have a very low sensitivity) and can potentially be loosened to achieve a cost reduction. Recall that there is typically a point at which looser tolerances doesn't improve cost because they have become so easy for the manufacturer to achieve. This result can also tell you if the design is simply unachievable with the current tolerancing scheme.

Zemax performs a sensitivity analysis with the following method:

- Nominal criterion is evaluated on the unperturbed system.
- The first operand is perturbed to the minimum tolerance value.
- The perturbed criterion is evaluated as a change from the unperturbed system.
- This process is repeated for the maximum tolerance value.
- This process is repeated for every tolerance operand within the Tolerance Data Editor table.

If the as-built optical performance is not adequate, then the designer will refer to the sensitivity analysis to determine the worst offenders. The worst offender tolerances are then reduced, if possible, and the process is repeated.

In our design Table 3 shows a worst offender table with only the axial alignment of Doublet 1 as the focus compensator. Because the chosen optical performance requirement is RMS WFE, the "Criterion" value must be less than 0.071 Wv. From the first tolerance analysis, 0.050 mm of decenter in doublets 1 (TEDR 10 12) or Double 2 (TEDR 15 17) impart roughly twice the RMS WFE to the system in the "Change" column. The following 3 surface and element tilts also consume most of the tolerance margin: those 3 RSS to 0.05 Wv RMS.

Table 3: Worst offender sensitivities with focus alignment.

Worst offenders:					
Type			Value	Criterion	Change
TEDR	15	17	0.05000000	0.15486203	0.15111343
TEDR	10	12	0.05000000	0.13453445	0.13020190
TSTX	16		0.05900000	0.04594889	0.03105350
TETX	10	12	0.03500000	0.04397300	0.02804716
TSTX	11		0.03500000	0.04328880	0.02696180

From the initial sensitivity analysis, it's clear that simply tightening tolerances is not adequate to meet requirements. Instead, we will attempt to use an element that is sensitive to radial runout to compensate for WFE for the tolerance stack-up in the remaining elements. The 2 obvious choices are Doublet 1 and Doublet 2. Doublet 1 is already being used as a focus compensator, so we will choose to add Doublet 2 as a compensator. For this a coordinate break is added around that element and Parameter 1 and 2 (X and Y decenter) are added as compensators.

Table 4 shows worst offenders after adding the doublet 2 compensator. The Change column now shows a more reasonable balance, which the highest contributor adding only ~0.01 Wv RMS.

Table 4: Worst offender sensitivities with focus alignment AND lateral alignment compensators.

Worst offenders:					
Type			Value	Criterion	Change
TIRR	12		-0.50000000	0.04112371	0.01037135
TIRR	5		0.50000000	0.03920656	0.00845420
TIRR	6		-0.50000000	0.03904741	0.00829504
TRAD	25	1	-0.50000000	0.03851628	0.00776392
TIRR	17		-0.50000000	0.03791502	0.00716265
TTHI	24	29	0.10000000	0.03752259	0.00677023
TIRR	11		1.00000000	0.03651035	0.00575799
TIRR	22		1.00000000	0.03591357	0.00516121
TIRR	10		0.50000000	0.03590613	0.00515377
TIRR	23		-1.00000000	0.03564827	0.00489591

Compensators are assumed to be alignments performed during the assembly of the system. For each of the compensators defined, we must define the range of motion necessary, and this must be accommodated by the available mechanical adjustment. Table 5we see the thickness compensator on Doublet-1 requires *at least* ± 0.5 mm of axial adjustment to maintain the required parfocal distance in assembly. In Table 6, we see that Doublet-2 requires *at least* 0.05 mm of radial clearance to compensate for optical performance.

Table 5: Compensator statistics for axial alignment compensator, Double-1.

Compensator Statistics:		
Thickness Surf 9:		
Nominal	:	0.003952
Minimum	:	-0.401829
Maximum	:	0.500162
Mean	:	0.033837
Standard Deviation :		0.181423

Table 6: Compensator statistics for lateral alignment compensator, Doublet-2.

Parameter 1 Surf 14:			Parameter 2 Surf 14:		
Nominal	:	0.000190	Nominal	:	-0.001735
Minimum	:	-0.053243	Minimum	:	-0.044538
Maximum	:	0.035265	Maximum	:	0.044533
Mean	:	0.000286	Mean	:	0.001096
Standard Deviation :		0.020002	Standard Deviation :		0.021486

The added complexity of the mechanical components needed to allow for the alignment should be considered in the overall impact of cost on the product. Other things to consider are the added labor to perform the alignment, tooling to mount and adjust the assembly, and additional metrology equipment to provide feedback. Additional compensators should only be added out of necessity, not just as a convenience to the designer.

65

5.d. As-Built Performance

As-built performance is the predicted performance of the system once it is manufactured and assembled. The as-built performance is a probability of a given assembly meeting the system performance requirements based on the Monte Carlo results (or some other statistical method). This could take the form of a sorted pareto of a given performance metric. Sorted pareto means the MC runs are sorted by the desired metric in ascending order prior to plotting the metric as a function of % yield. Zemax tolerancing returns the performance for several helpful yield levels.

```
90% >    0.06048320
80% >    0.05426294
50% >    0.04609530
20% >    0.03836365
10% >    0.03606374
```

Figure 47: Yield for 1x ZWF as reported by Zemax Tolerance Results.

There are several ways to define the expected as-built performance and what is required of a design. For low production, high inspection assemblies like this, 95% MC may be acceptable. The risk of escape is low because each unit is tested prior to shipping to a customer. For high-production assemblies, where 100% in-process testing is cost prohibitive, 99.7% MC or greater may be required.

So, the 1x ZWF optical design appears adequate. In the next section, we'll discuss in more detail what optomechanical considerations influence the tolerance scheme and mounting configurations necessary to achieve the chosen tolerances.

6. Optomechanical Design Basics

6.a. Integrated Optomechanical Design

Integrated optomechanical design means that the mechanical design requirements of the system should be considered during the optical design process. This goal of integrating this scope of work is to shorten the loop between optical and mechanical designers and to reduce design iterations. This should reduce the cost and labor to produce a design as well as reducing the risk of the design.

The considerations of this approach have been touched on throughout this paper but have not yet been explicitly stated. We have discussed primarily how the sensitivity of alignment tolerances will inform the optomechanical design about the allowable alignment methods. Several mounting and alignment methods are discussed below.

The tolerance scheme chosen should accurately reflect the chosen alignment strategy. When a lens can slide within a cell, the tolerances scheme should include this runout tolerance. When a lens instead rolls on its optical surface, the tolerance scheme should include a tilt tolerance about the center of curvature to accurately model that motion.

6.b. Optomechanical Mounting Methods

Here we'll outline several options for optomechanical mounting methods that may be employed. The mounting method is comprised of a few considerations; the assembly method, the surface contact interface, and any necessary alignment compensators.

b.1. Surface Contact Interfaces

When mounting an optic in an optomechanical assembly, the optic will generally come in direct contact with a metal housing, spacer, and/or retaining ring. The interface between these components contact surfaces often defines what tolerances schemes are appropriate.

There are many other methods to mount an optical element that are covered in other sources. Thes following are mentioned for being the most common and most relevant to the objective design at hand.

b.1.1. Sharp Contact

The metal cell forms a theoretically sharp corner, which contacts the surface of the lens on the optical surface, outside of the clear aperture. This method has a high surface contact stress from the sharp corner of the metal, so should be avoided for larger lenses. In practice, the lens is not a perfectly sharp corner, but has a slight chamfer or similar from post-processing such as deburring.
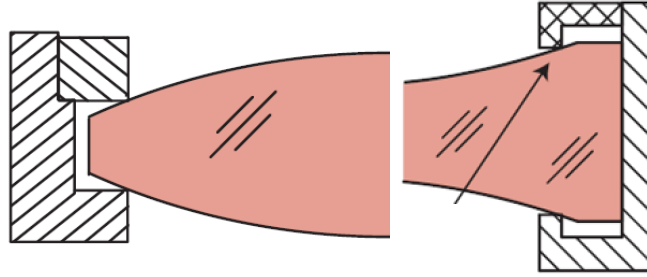
Figure 48: Sharp surface contact interface on convex (left) and concave (right) surfaces. (14)

The sharp contact surface interface can be a reasonably accurate alignment method depending on the geometry of the lenses and mounting mechanics. This is discussed in further detail in 6.c

b.1.2. *Flat-Bevel Contact*

Flat bevel contact is used for a concave surface. A flat bevel is ground into the edge of the surface to give a flat surface for the cell or retainer to contact. This is not a high precision method as the lens is generally allowed to contact the OD of the cell. The addition of the manufacturing step to grind a flat bevel adds an additional tolerance that needs to be considered.
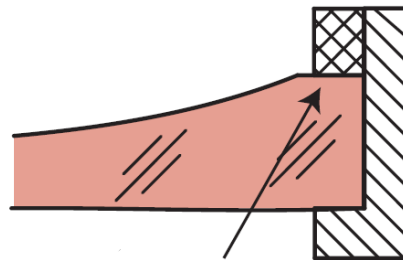
Figure 49: Flat surface contact interface. (14)

This is fundamentally the same type of contact as a plano optic, such as a QWP, would use with the obvious caveat that it is not necessary to grind a flat bevel onto the surface. The plano optic is simpler in that it is usually *entirely* insensitive to decenter.

68

b.1.3. *Tangential Contact*
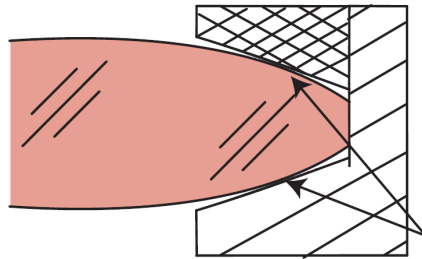
Figure 50: Tangential surface contact interface. (14)

b.1.4. *Floating*

For applications that are highly sensitive to strain, the optical element can be left 'floating' on adhesive. The element would be held in place and aligned as necessary with shims or other tooling. Adhesive is applied and allowed to cure before the shims or tooling is removed.

6.c. *Alignment Methods*

c.1. *Drop-in alignments*

In this case the lens is placed into a housing barrel and then constrained by either a threaded retaining ring or by a spacer in a stack of multiple lenses, the spacer being necessary to set the appropriate air space. This is the preferred alignment method if tolerances support it; the ease of assembly can keep costs down by minimizing labor. The runout or element roll is only controlled by the tolerances on the OD of the lens and the ID of the barrel. Controlling these very tightly can be impractically expensive.
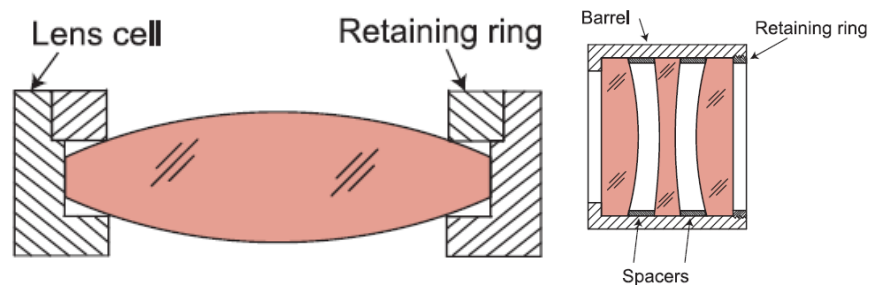
Figure 51: Lens in cell secured with retaining ring (left); multiple lenses stacked in a barrel, separated by spacers, and secured with a retaining ring (right). (14)

69

An alternative to the straight-barrel drop-in alignment is the stepped-barrel drop-in. In this method, each lens or lens group has a unique diameter, and the lens seats are machined directly into the housing. This is useful if the clear apertures vary significantly throughout the system. Each lens seat may house a single element, or a group of elements that have the same diameter and are separated by spacers.
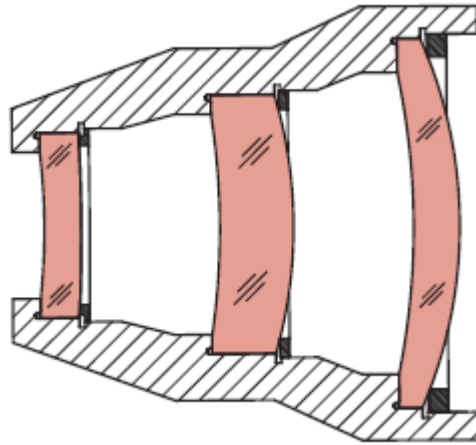
Figure 52: Lens barrel using stepped-diameter design. (14)

There is a limit to how much the lens can be constrained in this manner anyway as the radial gap must account for the thermal expansion and contraction of the glass and housing material to avoid unacceptable hoop stress on the lens. The radial clearance can be calculated as clearance = $(D/2)(\Delta T)(\alpha_c - \alpha_g)$, where α_i is the coefficient of thermal expansion. For example, when Schott N-BK7® (α = 7.1 x 10^{-6}/K)[vii] lens is potted within Aluminum (α = 23.1 x 10^{-6}/K)[viii], this works out to 16 x (D/2) (ΔT). For small lenses, this margin can be smaller than reasonable manufacturing tolerances for the components. The amount of thermal contraction and therefore, necessary clearance, scales with the lens mechanical semi-diameter of the materials.

[vii] https://www.schott.com/shop/medias/schott-datasheet-n-bk7-eng.pdf

[viii] https://www.engineeringtoolbox.com/linear-expansion-coefficients-d_95.html

70
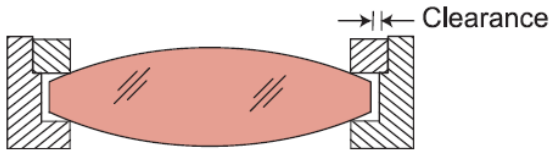
Figure 53: (14)

c.2. *Bell clamping*

There is an additional benefit in that the lens surfaces may be held in alignment by the force of the edge on the optical surfaces. That is, the lens is fully constrained by intersection of the circular edges and spherical surfaces. This benefit is limited to lenses where the clamping force can overcome friction between the cell and lens surface. This self-centering criterion is given by Yoder as;

$$\frac{\sin(\alpha)}{\cos(\alpha)} = \tan(\alpha) > \mu.$$

Where α is the clamping angle given by;

$$\alpha = \sin^{-1}\left(\frac{Y_{c1}}{R_1}\right) + \sin^{-1}\left(\frac{Y_{c2}}{R_2}\right)$$
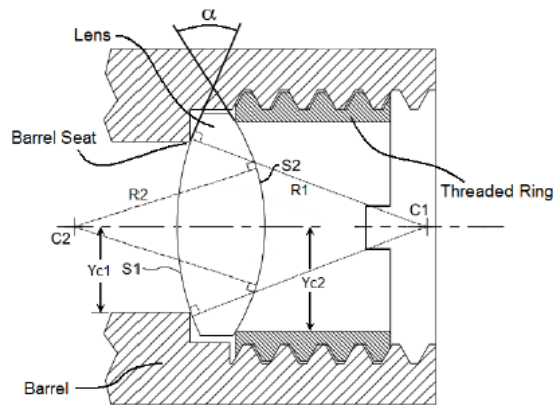
Figure 54: Parameters relevant to clamping angle of surface contacted lens. (15)

71
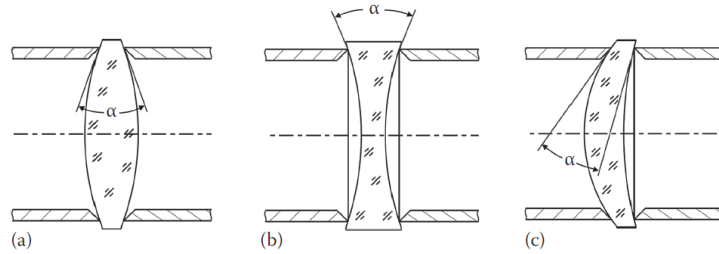
Figure 55: Clamping angle, α, for bi-concave (a), bi-convex (b), and positive meniscus (c) lenses. (15)

c.3. *Auto-Centering*

Another interesting technique is an auto-centering technique patented by Institut National d'Optique (INO). Publications from the inventor claim to achieve centering tolerances like active alignment (single-digit μm) with cost of labor like drop-in alignment. (16) This method involves a that is dropped into a cell and retained with a retaining ring, just like the drop-in method. However, the angle of the retaining ring threads is chosen to meet their auto-centering condition.
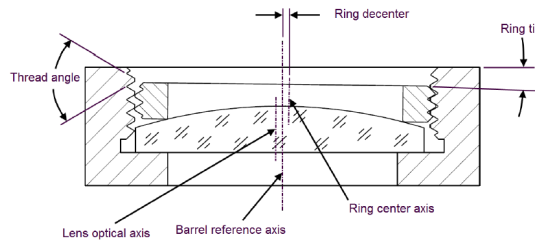
Figure 56: Typical lens alignment is sensitive to retaining ring centering error. The lens optical axis moves as the retaining ring is decentered. (17)
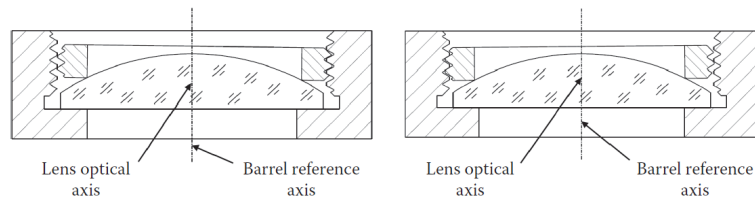
Figure 57: Auto-centered lens centration is insensitive to retaining ring centering error. The lens optical axis remains fixed as retaining ring is decentered. (17)

The inventors also claim that the concept of auto-centering is extensible to full optomechanical assemblies. For this, the cells and housing geometries need to be chosen to meet the auto-centering condition as well. An example of a full opto-mechanical assembly is shown in Figure 58, including an axial alignment between barrel 1 and Barrel 2.

72
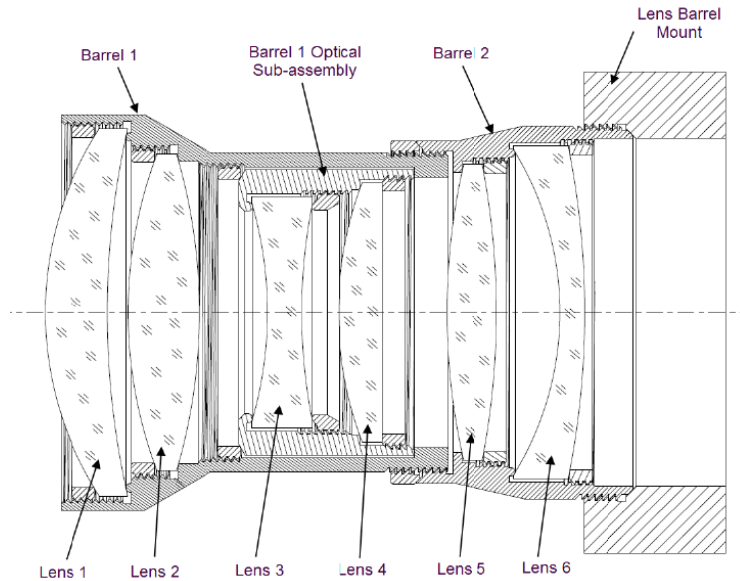
Figure 58: Auto-centered lens assembly. (17)

c.4. *Shim-centered*

In this method, a set of shims is used to achieve an even radial gap between the cell and lens. The lens is potted with adhesive, which is allowed to cure before the shims are removed. With well-selected shim thickness, the variation in radial clearance can be extremely small. In this way, the consistent radial clearance significantly reduces the radial runout or roll of which the lens is capable. The remaining tolerances to consider are the lens barrel centration error and the lens wedge.

The thickness of adhesive can be chosen to compensate for the thermal expansion of the glass and metal. This is given by Yoder as:

$$t_E = (D_G/2)(\alpha_M - \alpha_G) / (\alpha_E - \alpha_M),$$

Where αi is the CTE of the Metal, Glass, and Elastomer adhesive.

c.5. *Active Lens Alignment*

For even higher precision alignments, the lens will be actively centered within the cell. One method to perform this alignment includes a tool with an alignment telescope and a precision air-bearing rotation stage, such as a Trioptics OptiCentric or similar. The cell is aligned to the rotation axis of the air bearing by its mechanical datums using an indicator gauge. This rotation axis serves as the datum simulator for the optical axis of the lens. The

73

lens is then placed in the cell and centration is measured by observed a return from the surface with the alignment telescope as the stage is rotated. The lens can then be aligned to reduce the centration error.

This method is very precise but comes at a high cost. There is far more labor involved in aligning each cell and lens and waiting for adhesive to cure.

6.d. Alignment Errors

d.1. Barrel Error

In addition to the typical lens manufacturing errors, the optomechanical design must include possible errors within the mechanical components. The two primary errors are the decenter and tilt of the lens seat relative to the datum that defines the ideal optical axis of the system. A lens mounted as in Figure 59 would reasonably have a decenter tolerance to define the barrel concentricity, a tilt tolerance and a roll about the center of curvature of the bottom surface to fully describe the full possibility of mounting geometry errors.
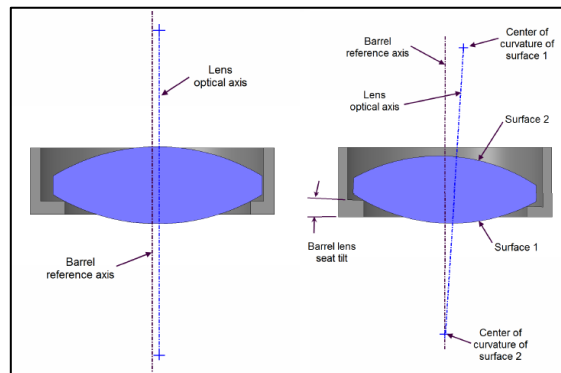
Figure 59: Geometry of Barrel Error due to decenter of the lens seat (left) and tilt of the lens seat (right)

6.e. Manufacturing Limits

When determining appropriate tolerance limits based on the chosen mounting configuration, it's important to understand manufacturing limits. This helps to inform the designer when a tightened tolerance will incur excessive cost by either requiring a more expensive fabrication method, reducing yield, or increasing assembly costs.

This is best accomplished by communicating with the intended manufacturers, but we've included sample manufacturing limits below. Optimax gives a useful table (Table 7 with manufacturing tolerances grouped into "commercial", "precision", and "high precision"

74

quality levels. The implication is that there is a step-function in cost when moving from one level to the next. Engineering Toolbox gives a summary of expected mechanical manufacturing tolerances based on fabrication process in Table 8 and Table 9. Higher precision processes are more expensive, as a rule.

Table 7: Optimax optical manufacturing tolerance chart[ix]

ATTRIBUTE	COMMERCIAL	PRECISION	HIGH PRECISION
Glass Material(n_d,V_d)	±0.001,± 0.8%	±0.0005, ±0.5%	Melt Rebalanced & Controlled
Diameter (mm)	±0.000/-0.100	±0.000/-0.025	±0.000/-0.010
Center Thickness (mm)	±0.150	±0.050	±0.020
SAG (mm)	±0.050	±0.025	±0.010
Clear Aperture	80%	90%	90%
Radius (larger of two)	±0.2% or 5 fr	±0.1% or 3 fr	±0.025% or 1 fr
Irregularity - Interferometer (waves, PV)	1	0.25	0.05
Irregularity - Profilometer (microns, PV)	±2	±.5	N/A
Irregularity - CMM (microns, PV)	±5	±1	N/A
Wedge Lens (ETD, mm)	0.05	0.01	0.005
Scratch Dig (ISO 10110-7:2017)*	80 - 50	60 - 40	10 - 5
Surface Roughness (Å rms)	20	10	5
AR Coating(RAve)	MgF2 R<1.5%	V-coat R<0.2%	Custom Design

Table 8: Machining process tolerance grades.[x]

Tolerance Grades									
4	5	6	7	8	9	10	11	12	13
Lapping and Honing									
	Cylindrical Grinding								
	Surface Grinding								
	Diamond Turning								
	Diamond Boring								
	Broaching								
		Reaming							
			Turning						
			Boring						
					Milling				
					Planning and Shaping				
					Drilling				

[ix] https://www.optimaxsi.com/charts/manufacturing-tolerance-chart/

[x]https://www.engineeringtoolbox.com/machine-processes-tolerance-grades-d_1367.html
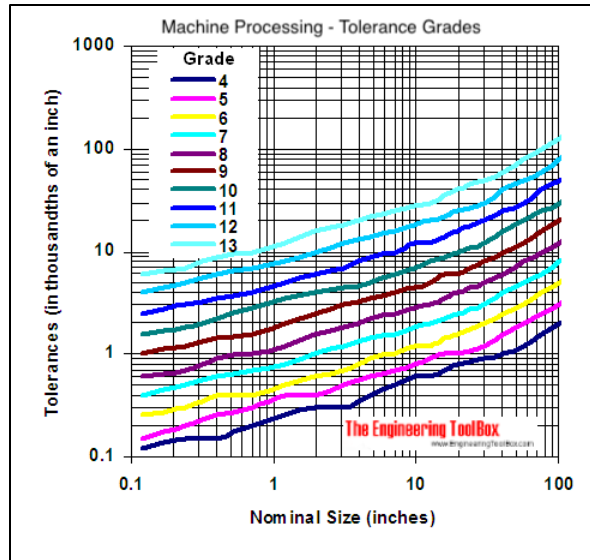
Figure 60: Standard machine tolerances by process grade per Table 10. [xi]

6.f. *Active System Alignment*

Here we'll refer to an active alignment as making an adjustment to lens position within the system based on feedback from some form of optical performance. For example, a system can be assembled and rough aligned using mechanical tolerancing before a final alignment step. Then, as a fine-alignment step, TWF (or some other metric) can be measured, and adjustments made to improve the performance until the criteria is met.

Everything identified as a compensator in section 0 should allow for active alignment during assembly or operation. Here we'll discuss the most common alignments and how they relate to the proposed 1x objective design.

f.1. *Axial alignments*

Almost all optical systems have some form of axial alignment; it is so common that the final airspace thickness is the default compensator in Zemax during tolerancing. In the case of imaging optics, there exists an optimal image plane out in object space. The final airspace compensator simply moves the detector plane to coincide with the image plane.

[xi] https://www.engineeringtoolbox.com/machine-processes-tolerance-grades-d_1367.html

76

Alternatively, a different element or group that has a sensitivity on the back focal distance can be used for axial alignment if the detector position is fixed. This sensitivity will show as a change in the focal plane position (which can be set as a compensator) as a function of the thickness (airspace or glass).

The need for axial alignment was identified during sensitivity analysis to maintain focus position within a reasonable parfocal range. Figure 61 demonstrates this sensitivity of the systems focus position to the axial position of doublet 1 (purple box).
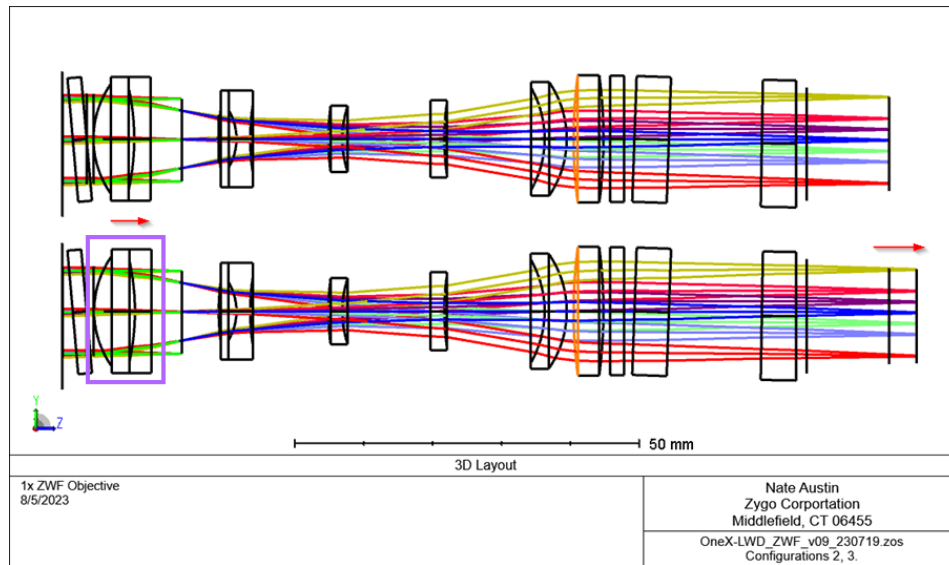
Figure 61: Diagram of 1x ZWF, shown at 1x system zoom, demonstrating sensitivity of image plane position on Doublet-1 axial position.

The doublet can be installed into a cell and captured with a retaining ring. Prior to installing the QWP, the cell is threaded into the housing to achieve the desired focus position and secured with a retaining ring. This adjustment requires at least ± 0.5 mm alignment range to accommodate the expected distribution of focus positions.

There is another need for axial alignment in the proposed 1x ZWF design. Once the position is defined for the imaging focus, set by Doublet-1 axial alignment, the interferometric focus must be set. This ensures that the reference surface is also in focus and that the fringe envelop lies within the depth of field of the object. This is required to perform surface topography with the optimal resolution. This alignment is discussed in further detail in section 7.f.

77

One common example is the zoom lens, in which 2 groups of lenses have a simultaneous axial alignment. One group has a sensitivity to the EFL of the lens system, while the other group has sensitivity to the focal plane position. The lenses are adjusted in concert along predetermined paths (usually machined into a cam-barrel) so that the image remains well-focused throughout the range of EFL adjustment. Our objective has a fixed focal length, so we don't need to consider this arrangement, but it's a good demonstration of the versatility of axial alignment.
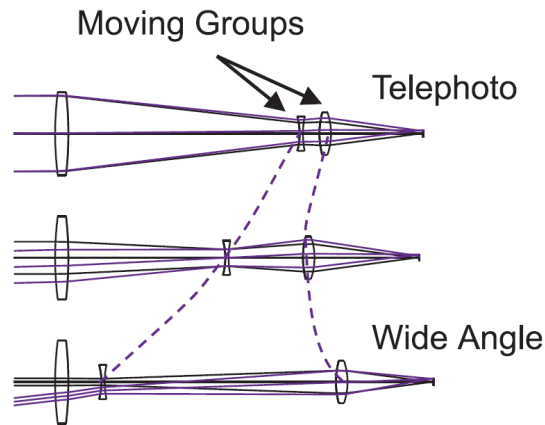
Figure 62: Example of zoom lens with 2 simultaneous axial alignments. (5)

f.2. *Lateral Alignment*

Lateral alignment of an individual lens or lens group may be necessary to compensate for off-axis errors within the system. Low order off-axis terms like astigmatism and coma generally have the largest contributions to optical performance, so they are typically compensated with lateral alignments to bring the system within performance requirements.

Some additional mechanical considerations are required. The lens or lens group is installed into a cell. The cell is installed in the housing such that it is captured with adequate preload, but also allowed to move during the alignment. The cell is pushed around with set screws that are threaded through the outer housing and contact the OD of the cell. The set screws are locked in place once final alignment is achieved, or the cell is potted in place with adhesive before removing the adjustment screws. Three screws allow for a kinematic movement but will couple X and Y-axis adjustments. Four screws will decouple X and Y-axis adjustments but may over-constrain the cell.

During sensitivity analysis, it was determined that the proposed 1x ZWF requires exactly this type of alignment. Doublet 2 must be laterally aligned to compensate for off-axis errors contributed by the rest of the as-built system, shown in Figure 63.
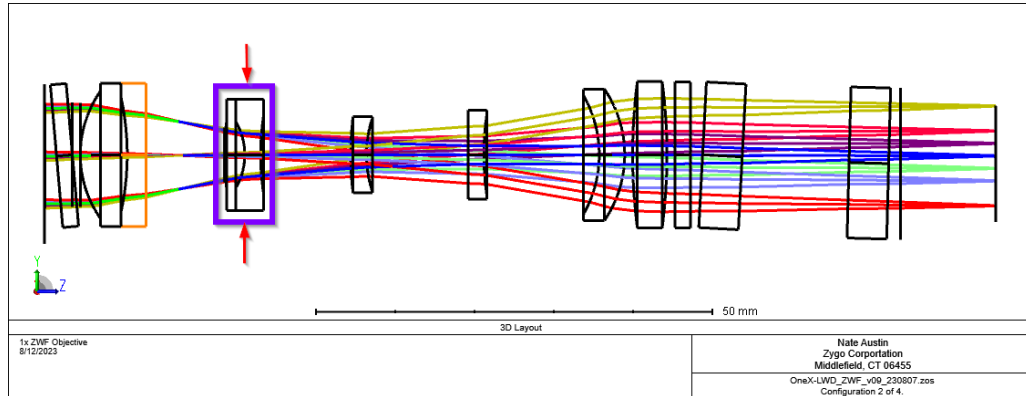
Figure 63: Diagram of 1x ZWF, shown at 1x system zoom, demonstrating sensitivity of image plane position on Doublet-1 axial position.

f.3. *Angular Alignment*

Like lateral alignment, angular alignment may be employed on a single lens or group to compensate for system aberrations. It also requires additional mechanical considerations, but this scheme is more difficult in practice. Unless the center of rotation is located at the vertex of the lens, then adjusting the tilt will cause an axial misalignment. So, this type of alignment can end up being a simultaneous tilt and focus alignment.

Additionally, the mechanical components must be carefully designed to allow rotation while preventing lateral displacement if there is also a sensitivity to that misalignment. Plano optics may have a sensitivity to tilt but not decenter. A spherical profile on the cell OD would allow rotation of the cell while maintaining constant centration.

Within the 1x ZWF, no angular alignment is necessary to achieve optical performance, however the interference cell has a critical angular alignment that is discussed further in 7.f

f.4. *Rotational Alignment*

Most optical components, such as lenses, windows, and mirrors, are rotationally symmetric. Therefore, rotational alignment is rarely necessary. One exception is for birefringent and other polarizing components, such as the waveplates used to mitigate ghost reflections discussed in section 2.p. The waveplates only need to be aligned relative to one

79

another to ensure the proper retardance for the reference and test legs to be passed through the PBS. The larger waveplate (Figure 38, Item 6) is more difficult to access, so we will choose to install that in an arbitrary orientation. The smaller waveplate (Figure 38, Item 2) is accessible from the exterior of the objective and will be aligned. If waveplate can be potted or retained in a cell and rotated until the return from the test and reference leg is maximized before being locked in place. Locking this in place with a set screw would be reasonable; a retaining ring may cause unwanted rotation and the QWP is not sensitive to any lateral displacement from the set screw. Any misalignment of the waveplates will lead to elliptical polarization and result in signal being rejected at the PBS.

7. Interference Cell

The interference of the ZWF objective and other interference objectives are the most critical components and therefore have special considerations. In this objective type, the interference cell will comprise 2 plane-parallel plates, shown in Figure 64: the Beamsplitter (BS, item 116) and Reference (Ref, item 104) plate. As mentioned, the BS plate is titled by at least the NA of the objective to reject any light passing through the reference plate after a single reflection from the BS. The Ref plate has exactly twice the tilt of the BS plate so that is in normal to the chief rays reflected from the BS plate. This way, light passing through the Ref plate after two reflections from the BS plate (and one reflection from the Ref plate) will be parallel to the illumination. Together with the interference cell, the test surface, with an equal OPD, comprise the interference cavity. The BS and Ref plates don't change the angle of the transmitted test leg. Instead, the angle of the surface under test is aligned by the operator to be parallel to the reference leg by reducing tilt fringes in the cavity.

We have not spent much time talking about them during the optical design process because the imaging performance is nearly insensitive to surface and alignment errors in those 2 parallel plates. The performance of the objective to perform reliable areal topography is, however, highly dependent on their quality and alignment. Here we will discuss considerations that are specific to the interference cell.
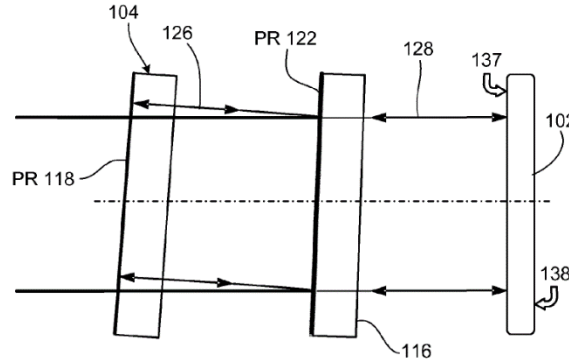
Figure 64: Figure showing ZWF interference cavity[xii].

7.a. Optical Coatings

The optical coatings on the BS and Ref define the intensity of the Test and Reference beams. The contrast of the fringes is defined by the visibility equation:

$$V = \frac{I_{max} - I_{min}}{I_{max} + I_{min}}; \quad I = I_1 + I_2 + 2 \cdot V(OPD) \cdot \sqrt{I_1 I_2} \cos(\Delta\phi)$$

Where V(OPD) is a visibility function due to temporal coherence of the source which creates the fringe envelope. The function is an inverse Fourier transform of the illumination spectrum (1), which is constant for monochromatic laser light and Gaussian for a Gaussian illumination profile.
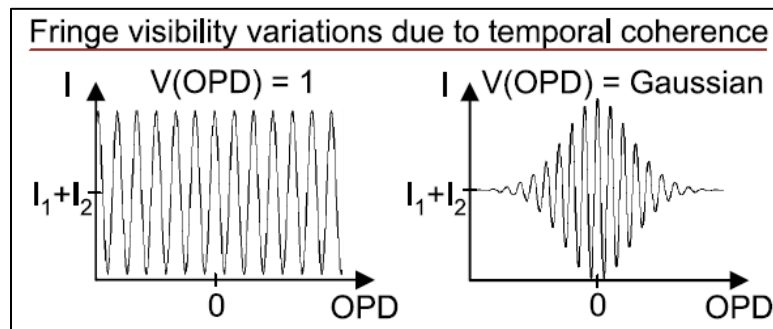
Figure 65: Fringe visibility due to temporal coherence, V(OPD). For a laser, this is approximately 1 (left) and for CSI, this can be approximated by a Gaussian function (right). (18)

[xii] Patent US 8,045,175
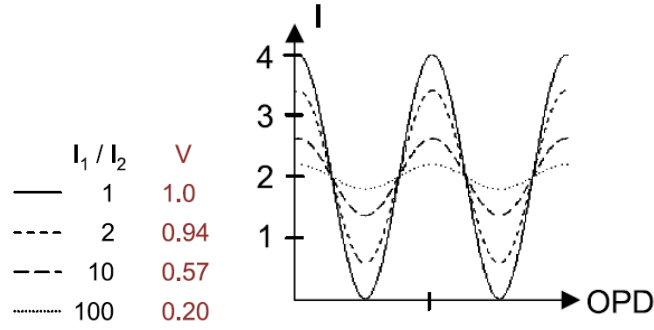
Figure 66: Fringe Visibility for various ratios of beam intensities. (18)

From the visibility equation, we can see that the maximum visibility is achieved when I_1 = I_2, so we will define optical coatings to achieve this condition with the FS test surface. When we trace the beam paths through the interference cavity, we see;

$$I_{REF} = R_{BS}^2 * R_{REF}; I_{TEST} = T_{BS}^2 * R_{TEST}$$

We desire to achieve the condition that $I_{REF} = I_{TEST}$, so;

$$R_{BS}^2 * R_{REF} = T_{BS}^2 * R_{TEST}$$

Due to the material choice to use **FS** as the **BS** and Ref plates, we've created a condition where $R_{TEST} = R_{REF}$ if the Ref plate is left uncoated. The equation above reduces to $R_{BS} = T_{BS}$. Therefore, the ideal BS coating is a 50% non-polarizing beam-splitter (NPBS).

7.b. Surface Irregularity and Power

Any figure error in the reference surface in this (and any interferometer) will directly add to the OPD of the reference leg and, therefore, represents measurement error of every measurement taken with the objective. To this end, the surface figure of reference surface is paramount. The surface of the beamsplitter is also non-common path. The reference leg is reflected from the reference surface twice, but the test leg is transmitted through the beamsplitter twice. These surfaces must be specified as tight as possible to provide the highest accuracy product to the customer.

For a coated, circular, plane-parallel plate, we expect the primary aberration to be power from the fabrication process or strain on the optic from the coating. Considering this, we could take some steps to help improve the manufacturability of the reference plates.

82

It turns out that we don't need perfectly flat plates, we just need the test beam to return on the same path on which it came. Because the reference leg bounces off the BS surface twice but the Ref surface once on the full round trip, it will return on the same path if the Ref surface has twice the power as the BS.

We could additionally specify a low-stress coating technology to avoid additional power due to strain on the BS surface (recall the Ref surface is uncoated in this implementation). Ion-Beam Deposition (IBD) creates dense coatings of very uniform thickness, but they tend to be high stress. Ion beam-assisted deposition (IBAD) would be more appropriate. In practice, we could simply control the power and irregularity of the surfaces and allow whoever is manufacturing the components to determine the most appropriate method to achieve those tolerances.

7.c. Plate Thickness

There are 2 specifications related to plate thickness that need to be considered to properly specify the components; overall plate thickness and plate thickness difference.

c.1. Overall Plate Thickness

The main consideration to determine the overall plate thickness, as it impacts the surface figure of the BS and Ref surfaces, is the self-weight deflection. This can be calculated analytically $\delta = Cq\frac{r^4}{D}$, where $D = \frac{Eh^3}{12(1-\nu^2)}$, C is dimensionless parameter related to mounting geometry, q is load per unit area, r is the plate radius, D is flexural rigidity of the plate, and ν is Poisson's ratio. Per Vukobratovich (19), for a plate of constant thickness this becomes:

$$\delta = C\left[\left(\frac{\rho}{E}\right)(1-\nu^2)\right]\left(\frac{r}{h}\right)^2 r^2$$

Self-weight can also be determined computationally through Finite Element Analysis (FEA). While the analytical approximation can provide a reasonable starting point, we'll rely on FEA to confirm the deflection meets the surface requirements. The figure below shows an example of the interference cell under static load of gravity with ring bond.
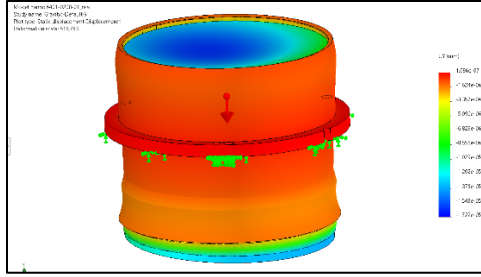
Figure 67: FEA of interference cell under 1 g static load.

Another thing that may impact the nominal plate thickness is the manufacturability. If the power and surface irregularity tolerances are very tight, the manufacturer may request that the plates be made thicker, so they maintain their shape better during polishing and coating. It's a good idea to communicate with potential suppliers on the manufacturability of critical components during the design process so that any changes can be considered and accommodated.

c.2. *Plate Thickness Difference*

It is known that a compensatory plate is required in a white-light interferometer. The compensatory plate is conveniently used as the reference plate in the ZWF objective. It is necessary due to the dispersion of the BS material. The requirement for a high contrast fringe envelope is that the OPD between test and reference legs be zero across the entire bandwidth; OPD(λ) = 0.

For this condition to be met, it is necessary that the material of the compensatory plate be very well matched to the BS plate in thickness, index, and dispersion. These requirements are typically far tighter than is possible to specify and achieve through typical process control. Instead, we could require that the plates are e.g., manufactured from the same melt of glass to ensure a match of index and dispersion and fabricated within the same batch to achieve a very small thickness difference.

7.d. *Plate Tilt*

In the ZWF interferometer, the plates are tilted with respect to the optical axis such that the reflections from the beamsplitter and reference plates fall are blocked at the aperture stop. To calculate this angle, we can use a couple convenient facts about the geometry of the system. The interference cavity occurs after all the imaging optics, so the ray angles (relative

84

to the optical axis) are the same at the plates as at the image. Also, this is a telecentric objective, so all the chief rays are parallel. These two features mean that any ray reflected outside of the numerical aperture (NA) of the objective will be blocked at the system stop.
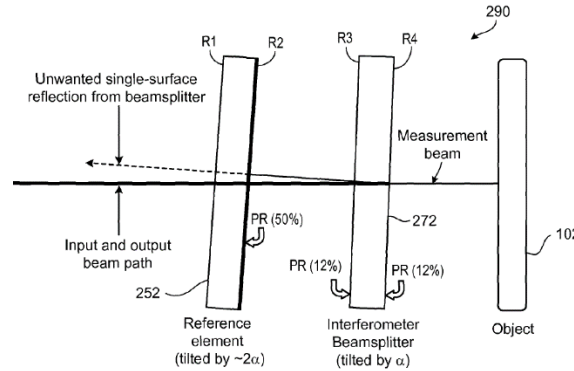
Figure 68: Diagram showing the source of the unwanted beam from BS surface.

We know the NA of the system is 0.030, so the half-angle is 1.7°. The BS plate must have *at least* this much tilt and the Ref plate will have exactly twice the tilt of the BS.
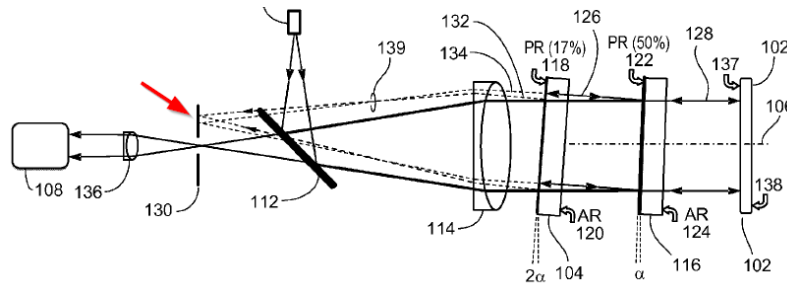
Figure 69: Profiler diagram illustrating returns from the Ref and BS surfaces are blocked when they fall outside of the numerical aperture of the objective.

7.e. Mounting

It should be clear that, due to the sensitivity of the BS and Ref surfaces to the performance of the objective, the mounting of those components is also critical. There are a few conditions that the mounting method should meet:

1. Mounting should be low strain to avoid imparting additional figure error to the BS and Ref plates after mounting.
2. Mounting should be athermal to avoid imparting additional strain throughout operating temperature range.
3. Mounting must be stiff enough to meet resonant frequency requirements.

85

4. Mounting must allow necessary alignments; see 7.f

e.1. *Proposed Mounting Configuration*

Here I propose we mount the Ref and BS plates into a single cell. The optics are floating, meaning that they are not in contact with the metal of the cell, and the adhesive thickness is chosen to create an athermal condition at nominal temperature. The cell has flexures to relieve strain at the bond pads and a flange to interface with the housing and allow necessary alignments, which are discussed in more detail in 7.f.

The interference cell subassembly can be modeled and analyzed using 3D CAD (Computer-Aided Design) software, such as SOLIDWORKS®, which is shown here. The Simulation add-on allows Finite Element Analysis (FEA), where a finite mesh of nodes representing the surface are perturbed to reveal mechanical properties of the assembly. In the following examples, I've used the model of the interference cell for the 0.5x ZWF that was mentioned earlier to perform additional analysis. Performing this scope of work for the 1x ZWF objective will be conducted as future work.
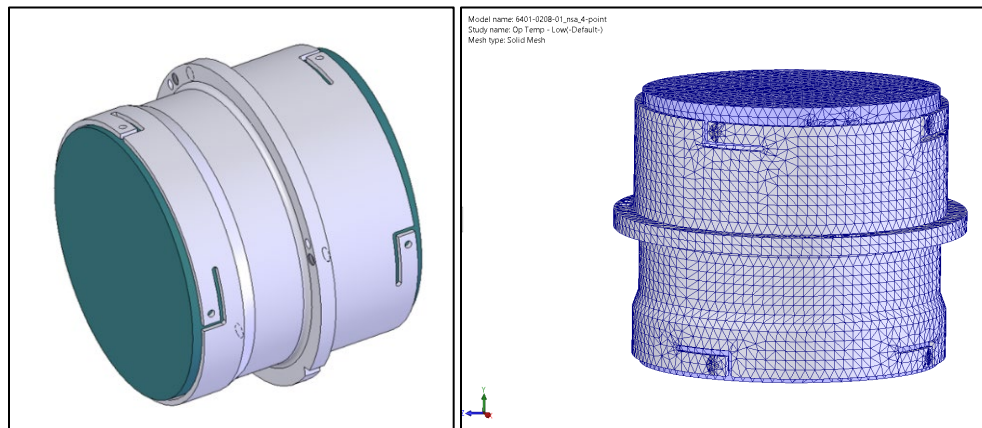
Figure 70: Figure of Interference Cell for 0.5x ZWF Objective (left) and the finite element mesh for FEA (right)

e.2. *Thermal Sensitivity*

Reducing strain induced on the reference surface due to thermal sensitivity is the main driver for the mounting configuration of these optics. As mentioned, the adhesive pad thickness is chosen to create an athermal condition and the flexures are meant to deflect instead of imparting stress to the optic.

86

Here we've used **SOLIDWORKS** to run a thermal **FEA** to show the strain due to changing the temperature from nominal (25° C) to minimum (15° C) and to maximum (30° C). The mesh of the resulting surface was then post-processed to yield a surface map that could be loaded in Zygo Mx software for further analysis.
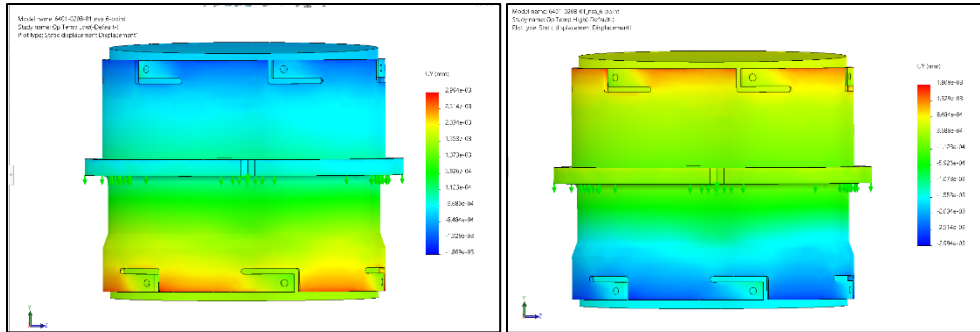
Figure 71: Thermal FEA from nominal temp to minimum (left) and maximum (right) operating temperatures.
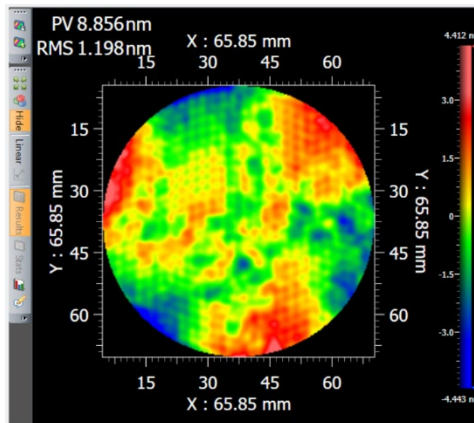
Figure 72: Surface deformation from thermal FEA. Surface mesh imported into Zygo Mx software for analysis.

The configuration shown above has already been optimized to yield an acceptable surface irregularity contribution throughout the operating temperature range, but that is not a guarantee. As an example of a mounting geometry that induces far too much strain on the Reference and BS optics throughout, I've modeled this subassembly using a ring-bond. In this configuration, the plates are still floating and not in contact with the cell. The bond-line is in the form of a ring that fills the gap between the plate and cell so that the stress applied is uniform around the optic. The resulting surface deformation exceeds the entire tolerance budget for the reference surface irregularity at either end of the operating temperature range.

87
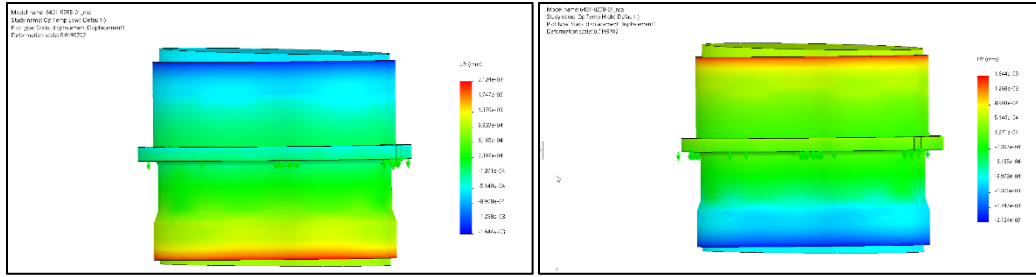
Figure 73: Thermal FEA of interference cell using ring bond.

e.3. *Vibration Analysis*

We've already shown that the mounting method does not induce undue thermal stress. In the absence of a stiffness requirement, mitigating thermal stress becomes trivial. In order to show that the mounting method is also stiff enough to support the resonant frequency requirement, we must perform resonant frequency FEA. The vibration FEA reports the modes of the lowest resonant frequencies of the assembly and demonstrates their shape. In the case of the 0.5x ZWF interference cavity, the primary mode is an oscillation of both plates simultaneously moving along the optical axis at 868.5 Hz. This is a great result and will not limit the resonant frequency of the full objective.
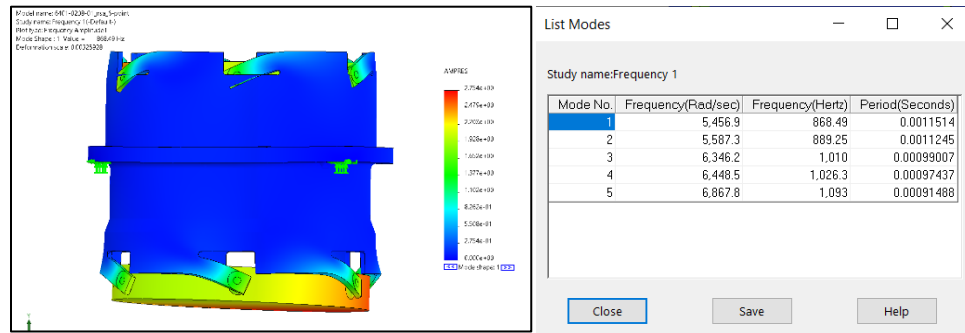
Figure 74: Resonant frequency FEA of interference cell showing the primary mode (left) and first five frequencies (right)

e.4. *Adhesive Choice*

For the analysis above, we've used a stiff 2-part epoxy, 3M™ Scotch-Weld™ Epoxy Adhesive 2216 B/A Gray, which has a shear strength of 49580 lb./in² at room temperature[xiii].

[xiii] https://technicaldatasheets.3m.com/en_US?pif=000157

88

The flexure mount has provided adequate compliance to avoid undue strain on the optic and the flexure and adhesive are both shown to be adequately stiff to meet resonant frequency requirements. Obviously, there are many adhesive choices, and they play a huge role in the optomechanical performance of the system. As an example, we've repeated the resonant frequency FEA with SNAPSIL™ RTV142 Adhesive Sealant, which has a shear strength of 300 lb./in² at room temperature[xiv].

The results show that the resonant frequency of the interference cell no longer supports the required system resonant frequency at 170 Hz.
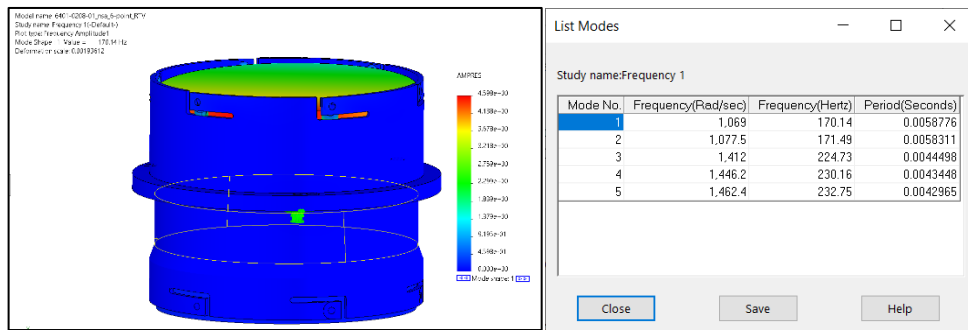
Figure 75: Resonant frequency FEA results with RTV142

7.f. *Alignment*

The interference cell mounting must allow precision angular and axial alignments.

Axial alignment is required to achieve a zero-OPD condition between the reference and test legs. The angular alignment of the interference cavity defines the plane in object space that achieves constant OPD across the field. If the cavity has tilt the test arm is returned through the objective at an angle relative to the optical axis. To achieve constant OPD with a tilted interference cell, then the object would need to have an equal amount of tilt, so the test and reference legs are parallel.

We'll instead align the cell to a very high degree of accuracy. This will ensure that the constant OPD condition held across the field overlaps the imaging object plane. It will also minimize the tilt between objectives and improve the customer experience when utilizing

---

[xiv] https://www.momentive.com/en-us/categories/adhesives-and-sealants/rtv142

turret-mounted objectives. To achieve this, and to compensate for possible boresight error in the objective, we will be incorporating an active alignment into the assembly process.

f.1. *Course Angular Alignment*

The first angular alignment that must be set is the tilt between the reference and beamsplitter plates. Because we're allowing an active alignment in a later step, this can be a "rough" alignment and achieved with appropriately toleranced tooling. I say "rough" because there is a relatively finer alignment step later in the process, but we will still attempt to align as well as we can at this point to reduce the labor of performing later alignment.

As mentioned, the potting sets the angle between the Ref and BS plate. This is a fixed value once the plates are patted. We are trying pot the plates such that this angle is equal to the angle between the BS and mechanical datum. The difference between these two angles is what will be aligned out in the final cavity tilt step.

Also worth noting, that the tilt in the plates must be in the same orientation for the objective to function. Clocking the cell while potting the plates must be considered when creating tooling.

f.1. *Axial Alignment*

Now that the lenses are potted into a cell, we can install the cell into the housing. This can be done by threading the cell into the housing and securing it with a lock ring. The reference surface will be threaded until it is located at the secondary object plane (reflected from the BS). This alignment can be performed on a wavelength-shifting laser interferometer, such as the Zygo Verifire™ MST to measure the power in the wavefront. We expect the plane parallel plates to cause internal Fizeau cavities that will disrupt phase-shifting measurements.

The objective has some non-zero longitudinal chromatic aberration as well as field curvature. At the point of best focus, we expect a range of power values as a function of wavelength and possibly some defocus to balance the best focus position across the field. When we set the nominal power at a single wavelength (as in a laser interferometer), we would want to offset the alignment by the amount of power in the system at that wavelength. When evaluated on-axis at test wavelength,
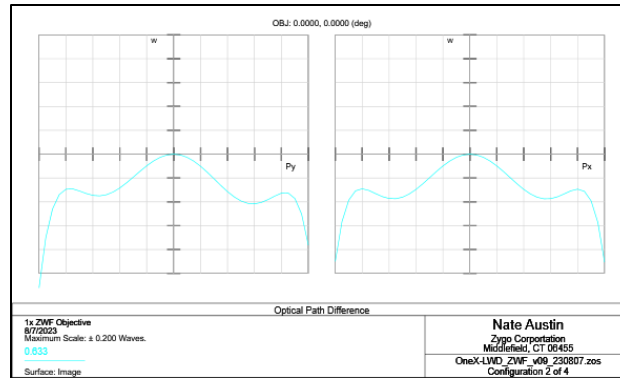
Figure 76: OPD on-axis at HeNe showing a negative power bias.

f.2. *Final Cavity Tilt and Focus*

Next, the tilt must be adjusted within the objective. A set of three kinematic set screws threaded through the flange we designed into the lens cell and contacting the housing may define the alignment plane. They could be paired with three screws that pass through the flange and thread into the housing to lock the cell in place. This arrangement allows for angular adjustment but is coupled with an axial adjustment because the center of rotation is not at the center of the rotation.

The cavity could be created with a tooling flat known to be well aligned to the system (objective and profiler). The fringes would provide the necessary alignment feedback to align the reference leg return.

There may be mounting configurations that decouple these axes, but they may also be more complicated to manufacture and less robust. We'll just resolve to perform a final cavity tilt and focus alignment concurrently.

8. Validation Testing

One more activity the optomechanical engineer should perform is developing the test plan and generating reasonable assembly tolerances. It's likely that two test plans are developed; a validation test plan and production test plan. The validation test plan would be an extensive bevy of tests performed by engineering as necessary to qualify the design to meet all parameters in the product requirement table. These tests will also qualify production methods and tooling are able to support the tolerances defined. This amount of testing is

91

obviously not tenable to perform on each objective that is assembled. The production test plan is a reduced set of testing as necessary to balance labor and risk to product quality.

Now that a fully toleranced optomechanical model has been developed, the acceptance tests may differ from the metrics that were used to optimize the model. If so, the acceptance test requirement should now be evaluated from the toleranced model.

For example, we chose RMS wavefront for our optical performance metric. However, performing a TWF measurement at a significant number of field points would be highly labor intensive and require specialized tooling. It would be more practical to measure the imaging performance directly as an Instrument Transfer Function (ITF).

The designed test may intend to use a sharp step-height feature to analyze Instrument Edge Spread Function (IESF) along one axis of the detector. The frequency content in each linear slice across the step is limited by the system ITF at that point. The slices across the step feature are averaged together, possibly across the entire detector.
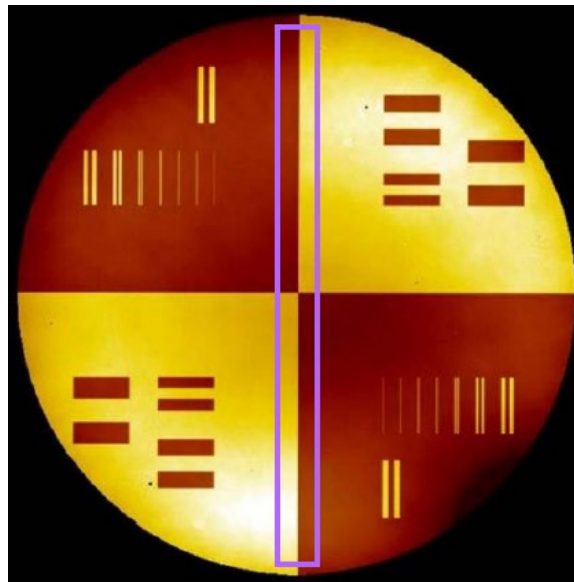
Figure 77: Phase map of sharp step-height feature showing the extent of the field averaged along a single axis. (9)
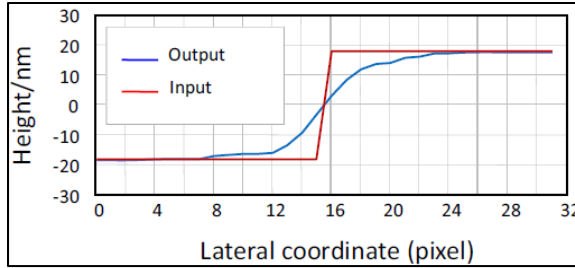
Figure 78: Graph of the ideal height of linear slice of a sharp step-height standard (red) and a possible real measured step which is limited by the line spread function of the system at that point (blue). (9)

This result is not something that was used during the design of the objective. To determine the expected ITF results using the IESF, the toleranced model Merit Function must be set to approximate the test conditions and then repeat the MC tolerancing run.

Table 9: Merit Function Editor setup to report the average MTF at a given spatial frequency across 5 field points.

9. Conclusions

In this paper we discuss elements of Optomechanical Design as they relate to the design of a 1x ZWF interference objective. We review details on the motivation for many of the system requirements. As we progress through the design process, we stress understanding the optimization operands that compose the Merit Function used to optimize the nominal design. We similarly discussed Tolerance Operands and stress structuring the Tolerance scheme to replicate the physical motion of optics as they are constrained by the mechanics. We then detailed several relevant alignment methods that may be used and stress identifying the mounting method for proper tolerancing. We then go into detail on the interference cell, which is a critical component of the objective.

93

APPENDIX A.   Optimization

Optimization is an iterative process wherein the starting design is molded into the final design. A MF is created to quantify the fitness of the current design and lens variables are adjusted by the lens design software.

a.1.   *Merit Function*

We're using Ansys Zemax OpticStudio, so this section will include the optimization operands (within the Merit Function Editor) that were used to meet the requirements listed above. As mentioned, it is vital to understand the operands that are being applied during optimization to ensure that the design space is properly constrained. A summary of several useful optimization operands can be found in APPENDIX B.

There is (almost always) more than one way to build a MF to achieve the same or similar constraints during the design process. Additionally, the MF will evolve as the design phase progresses. New operands are added (maybe as the result of the previous optimization causing the system to 'walk away'), operand weighting is shifted to prioritize different aspects of the design, and target values are changed as the design is 'messaged', for example.

a.2.   *Optimization Algorithms*

Once the Merit Function is defined, the lens is optimized using one of the Optimize functions. If the resulting design does not meet performance requirements, then either Merit Function is updated/reweighted, or the lens is altered to enter a difference solution space. Lenses can be added or subtracted, or any lens data parameters can be altered. Understanding the art of massaging an optical design goes beyond the scope of this paper and is left as an exercise for the reader.

There are 3 optimization operations available in Zemax. They can be used effectively in conjunction, such as (1) Optimize, (2) Global Search, then (3) Hammer Current on several Global Search output files.

a.2.1.   *Optimize!*

Optimizes to reduce MF to local minimum using (typically) Damped Least Squares. It can provide a quick optimization solution and is executed after nearly every change to the lens data table.

a.2.2. *Hammer Current*

Hammer can be used to escape local minima. It takes longer than the Optimize! algorithm.

a.2.3. *Global Search*

Global iteratively searches for the lowest MF in the solution space and saves the lowest MF solutions found. This is time and processor intensive. It's not uncommon to allow Global Search to run overnight.

APPENDIX B. Useful Zemax Optimization Operands

Here we will give a brief overview of some of the operands that were used to finalize the optimization of the subject design. This is not a complete list of operands used throughout the design process, nor is it the only reasonable set of operands to use based on the given objective performance requirements.

1. EFFL – Effective Focal Length

As mentioned in the previous section, the effective focal length of the objective defines its magnification. Magnification, being the defining characteristic of a microscope objective, the importance of controlling EFFL cannot be understated.

2. RAID – Real Ray Angle of Incidence in Degrees

This operand gives the angle of incidence in degrees relative to the surface normal. There are several operands that control ray angles in degrees or radians or cosines of angles relative to either the incidence surface, exiting surface, or optical axis. I will not go over them all, but they may all be adequate within this design. I simply prefer RAID.

This operand is used to control the ray angle of chief ray for several field points to be zero relative to the surface normal of the object. A chief ray is any ray from the center of the pupil, so $Px = Py = 0$. For the chief ray to emerge from the system parallel to the optical axis, the system must be telecentric. The position of the system stop must be allowed to float to satisfy the condition of telecentricity.

For an ideal system, it's only necessary to solve this constraint for a single field point. In real systems, pupil aberrations cause a variation in the chief ray angle across the field. I've used several field points to best balance the telecentricity.

There's also the option of setting the system up within Zemax such that the object space is telecentric and select that setting from the System Explorer > Aperture menu. In that case, we would also utilize the Afocal Image Space setting because we require this to be an infinity corrected objective.

3. DIMX – Distortion Maximum

This is a straightforward operand that sets the maximum distortion.

96

While Zemax help mentions that this operand is not valid for non-rotationally symmetric system, we're assuming that this design is close enough to rotationally symmetric for this operand to remain valid.

4. Material Thickness Constraints
    a. MNCA – Minimum Center Thickness of Air
    b. MXCA – Maximum Center Thickness of Air
    c. MNCG - Minimum Center Thickness of Glass
    d. MXCG - Maximum Center Thickness of Glass

These apply boundary values to the optical design center thicknesses of glass and air. These are necessary to ensure the solution is physically possible. Without these operands set to reasonable values, it's likely that optimization will return non-physical solutions, or maybe just completely unreasonable ones. These include air spaces/glass thicknesses that go negative or lenses that get unreasonably thick or thin.

They are so critical that they are offered to be automatically added to the MF through the Merit Function Editor Optimization Wizard and should always be applied with reasonable values. Ensure that dummy surfaces are not constrained to the same thickness range as actual airspaces.
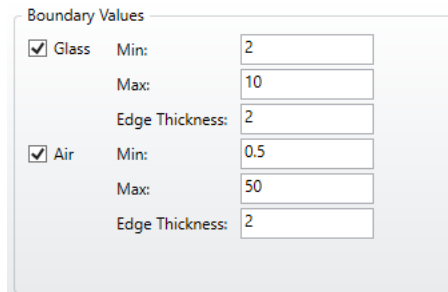
Figure 79: Boundary Values toolbox from Zemax Optimization Wizard

    e. MNEA – Minimum Edge Thickness of Air
    f. MNEG – Minimum Edge Thickness of Glass

These operands apply boundary conditions to the thickness at the edge of surface. Consider sequential concave surfaces; the center thickness of the air space may meet the

required boundary value set by MNCA, but due to the surface sag the thickness at the edge of the part may be less than zero. This is a non-physical solution to the design parameters.

The Max value boundary operands (MXEA, MXEG) are often not critical. A larger edge thickness of air or glass won't create a non-physical solution and they are often controlled through other more appropriate constraints.

5. CTVA – Center Thickness Value

This operand sets a thickness value for the given surface. You can think of this, if you like, as applying MNCA/G and MXCA/G simultaneously for the same boundary value. In the general case, when the desired thickness of a given surface is known, it is simply entered into the Lens Data table as a fixed thickness. However, when that thickness is the result of a solve (e.g., pickup, compensator, etc.), this operand is useful to constrain the contributors to that solve. In our case, CTVA was used to set the parfocal length of the objective. The parfocal length was included in the Lens Data as a Position Thickness solve from the mechanical shoulder surface through the object plane, and the sum of all surface thicknesses within that range is being constrained.

APPENDIX C.   Useful Zemax Tolerance Operands

1. TWAV – Test Wavelength

The Test Wavelength defined within the Tolerance Data Editor sets the test wavelength for other tolerances that are given in fringes or waves. For example, **TFRN** and **TIRR** are given in units of fringes. This wavelength may be distinct from the system design wavelength. If a HeNe-based Fizeau interferometer will be used for surface metrology, which is very typical, then the test wavelength should be 0.633 μm.

2. TFRN/TRAD - Tolerance on surface radius of curvature in fringes/lens units
   a. Spherical Surfaces:

When a spherical surface is being checked against a test plate, it is placed in direct contact with the surface of a tool with a well-known, calibrated surface curvature. It is illuminated with a Helium light source. Interference fringes in the form of Newton's Rings are observed when there is a difference in radius. The number of rings observed gives an approximate value for this difference in surface sag out to the edge of the part. The radius departure is a derived value from the nominal radius of curvature and the mechanical semi-diameter of the part under test. This gives a very fast and, therefore, cheap test that is often adequate for "commercial" grade optics. When designing commercial optics, it is advised to confirm the test plates available at the intended supplier and limit as many surfaces to those values as possible. This will cut down on the need to procure additional test plates, which typically cost well over $10k each and will add to the quote as a Non-Recurring Engineering (NRE) or Tooling charge or simply amortized across the quoted lot of parts (depending on how the supplier structures their quotes).
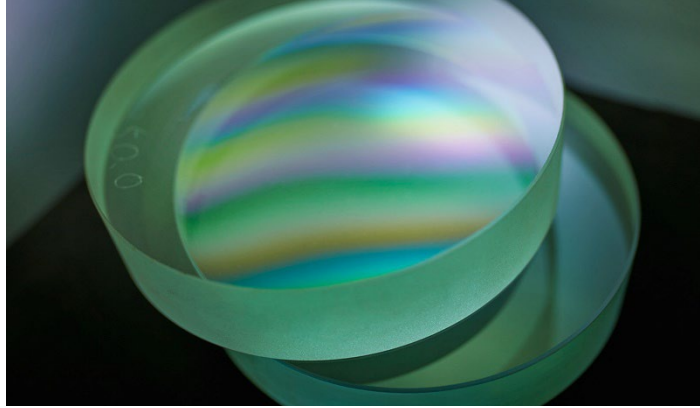
Figure 80: Test plating an optic showing interference fringes. [xv]

When dealing with "precision" optics, this may no longer be an adequate test method; a higher precision and, therefore, costlier test method is required. The term "Precision" is vague, but for the purpose of this paragraph we'll define to mean "An optic whose radius tolerance cannot be reliably measured against a test plate". For precision optics, testing on an interferometer with an Interferometric Radius Scale is required for the necessary precision. The distance measured on a Displacement Measuring Interferometer as the test surface moves from a Confocal to Cat's-eye cavity configuration is a direct measurement of the radius of curvature of the surface and has a precision typically < 100 ppm. Other commercial solutions utilize an Encoded Radius Slide for measuring the displacement of the optic during test. For precision optical surfaces, therefore, we can specify the radius tolerance directly in lens units (TRAD) and do not need to restrict the design to any set of pre-existing test plates.

[xv] https://www.tamron.com/global/monozukuri/waza/genki/

100
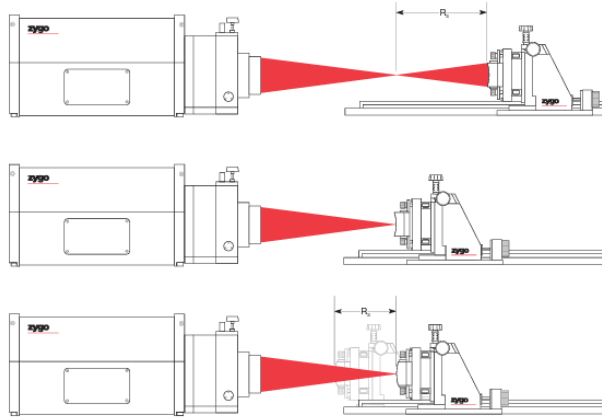
Figure 81: Interferometer test configuration for measuring RoC; a concave surface at confocal position (top), a concave surface after being translated to cat's-eye (middle), and a convex surface with both cat's eye and confocal positions superimposed (bottom).

b. Plano Surfaces:

Plano surfaces may also have a radius tolerance, even though the nominal radius is infinite. The measured value is the power term of the surface. Using lens units in this case is meaningless. What does Infinity +/- 5 mm mean? Specifying a surface sag via TFRN does have a physical meaning and will reliably control the amount of power in plano surface.

A plano surface that has power in it will contribute some amount of defocus to the overall system. This can typically be compensated for by adequate focus adjustment in the system, like the radius tolerances for spherical optics. When the typical plano surface is specified, the radius tolerance and surface irregularity tolerance are specified as two independent tolerances. When the surface is measured for conformance to those specifications, typically via Fizeau Interferometer, an amount of power up to the surface power specification must be removed prior to evaluating surface irregularity.

There are rare cases where this is not the case, such as the reference and beamsplitter surfaces within an interferometric metrology instrument. In that case, the surface power is not able to be compensated. Instead, it contributes to the interferometric cavity OPD and is therefore reported as surface error by the instrument. Since this is an interferometric objective, this system does have a reference and a beamsplitter surface.

3. TTHI – Tolerance on Thickness

101

Tolerance on thickness controls the center thickness of each element and airspace that it's applied to. The center thickness along the optical axis of the element is controlled during manufacturing by measuring with a drop-gauge or some similar instrument. The airspaces within the system are generally controlled by mechanical tolerances of e.g. spacers, cells, and housings.

It's critical to define how a thickness perturbation will impact the rest of the system. If, for example the assembly is a fairly simple 'stacked' configuration, separated by spacers that contact each lens, then each thickness perturbation will propagate through the stack. Alternatively, if each lens sits on its own machined surface within the lens housing, then the thickness perturbation of a given lens will not propagate to subsequent lens position. Instead, the position each lens will only be dependent on the mechanical tolerances of those lens seats.

These two contrasting tolerance stack-up paradigms are not mutually exclusive and will often occur within a single system, such as the 1x ZWF objective under discussion. Within Zemax, the tolerance control "Adjust" sets which airspace accommodates the perturbation of a given thickness tolerance. That is, a change in lens/airspace thickness of a given surface will cause an equal and opposite change in the Adjust surface identified.

4. TIND/TABB – Tolerance on index of refraction and Abbe number of an optical material

The material property tolerances for index of refraction (n_d) and Abbe number (v_d) must be specified for each element within the system. Many material suppliers publish their material grades within their e.g. optical glass catalog. This will give a reasonable starting point as it does not save any cost to specify something looser than the material supplier's lowest grade. The grades that are available to choose from is also dependent on the type of material chosen such as optical glass, fused silica, or more exotic crystals or ceramics.

Table 10: Standard material grades for Schott optical glasses.

	n_d	v_d
Step 0.5*	±0.0001 (NP010)	±0.1% (AN1)
Step 1	±0.0002 (NP020)	±0.2% (AN2)
Step 2	±0.0003 (NP030)	±0.3% (AN3)
Step 3	±0.0005 (NP050)	±0.5% (AN5)

References

1. **de Groot, Peter.** Coherence Scanning Interferometry. [ed.] Richard Leach. *Optical Measurement of Surface Topography.* Berlin/Heidelberg : Springer-Verlag, 2011, 9.

2. *The Relative Motion of the Earth and the Luminiferous Ether.* **Michelson, Albert A.** 1881, American Journal of Science, Vol. 22, pp. 120-129.

3. *A new class of wide-field objectives for 3D interference microscopy.* **de Groot, Peter J. and Biegen, James F.** Munich : Society of Photo-Optical Instrumentation Engineers, 2015. Proceedings of SPIE. Vol. 9525.

4. **de Groot, Peter.** Phase Shifting Interferometry. [ed.] Richard Leach. *Optical Measurement of Surface Topography.* Berlin/Heidelberg : Springer-Verlag, 2011, 8.

5. **Bentley, Julie and Olson, Craig.** *Field Guide to Lens Design.* [ed.] John E. Greivenkamp. Bellingham : Society of Photo-Optical Instrumentation Engineers, 2012. Vol. FG27. ISBN 978-0-8194-9164-0.

6. *Systematic Design of Microscope Objectives; Part II: Lens Modules and Design Principles.* **Zhang, Yueqian and Gross, Herbert.** 5, s.l. : De Gruyter, 2019, Advanced Optical Techniques, Vol. 8, pp. 349–384.

7. *PVr—A Robust Amplitude Parameter for Optical Surface Specification.* **Evans, Chris J.** 4, s.l. : Society of Photo-Optical Instrumentation Engineers, 2009, Optical Engineering, Vol. 48.

8. *Accurate Calculation of Diffraction-Limited Encircled and Ensquared Energy.* **Anderson, Torben B.** 25, s.l. : Optical Society of America, 2015, Applied Optics, Vol. 54, pp. 7525 - 7533.

9. *The instrument transfer function for optical measurements of surface topography.* **de Groot, Peter J.** 024004, s.l. : IOP Publishing Ltd, 2021, Journal of Physics: Photonics, Vol. 3.

10. *Computer-simulation analysis of ghost images in photographic objectives.* **Kojima, Tadashi, Matsumaru, Takashi and Banno, Makoto.** s.l. : Society of Photo-Optical Instrumentation Engineersv, 1980. Proceedings of SPIE. Vol. 0237, pp. 504 - 509.

11. *Deep learning-enabled framework for automatic lens design starting point generation.* CÔTÉ, GEOFFROI, LALONDE, JEAN-FRANÇOIS and THIBAULT, SIMON. 3, s.l. : Optical Society of America, 2021, Optics Express, Vol. 29, pp. 3841 - 3854.

12. *Optical Design at The Age of AI.* Thibault, Simon, et al. 03023, s.l. : EDP Sciences, 2022, The European Physical Journal Conferences, Vol. 266.

13. Lamontagne, Frédéric. Optomechanical Tolerancing and Error Budgets. [ed.] Anees Ahmad. *Handbook of Optomechanical Engineering.* Boca Raton : Taylor & Francis Group, LLC, 2017, 7.

14. Schwertz, Katie and Burge, James H. *Field Guide to Optomechanical Design and Analysis.* [ed.] John E. Greivenkamp. Bellingham : Society of Photo-Optical Instrumentation Engineers, 2012. Vol. FG26. ISBN 978-0-8194-9161-9.

15. Yoder, Paul R. Jr. and Frédéric Lamontagne. Optical Mounts; Lenses, Windows, Small Mirrors and Prisms. [ed.] Anees Ahmad. *Handbook of Optomechanical Engineering.* Boca Raton : Taylor & Francis Group, LLC, 2017, 8.

16. *Disruptive advancement in precision lens mounting.* Lamontagne, Frédéric, et al. s.l. : Society of Photo-Optical Instrumentation Engineers, 2015. Proceedings of SPIE. Vol. 9582.

17. *High precision optomechanical assembly using threads as mechanical reference.* Lamontagne, Frédéric, et al. s.l. : Society of Photo-Optical Instrumentation Engineers, 2016. Proceedings of SPIE. Vol. 9951.

18. Goodwin, Eric P. and Wyant, James C. *Field Guide to Interferometric Optical Testing.* [ed.] John E. Greivenkamp. Bellingham : Society of Photo-Optical Instrumentation Engineers, 2006. Vol. FG10.

19. Vukobratovich, Daniel. Optomechanical Design Principles. [ed.] Anees Ahmad. *Handbook of Optomechanical Engineering.* Boca Raton : Taylor & Francis Group, LLC, 2017, 2.

20. Geary, Joseph M. *Introduction to Optical Testing.* Bellingham : SPIE—The International Society for Optical Engineering, 1993. ISBN 0-8194-1377-1.

21. *Systematic Design of Microscope Objectives; Part I: System Review and Analysis.* **Zhang, Yueqian and Gross, Herbert.** 5, s.l. : De Gruyter, 2019, Advanced Optical Techniques, Vol. 8, pp. 313–347.

22. *Systematic Design of Microscope Objectives; Part III: Miscelaneous Design Principles and System Synthesis.* **Zhang, Yueqian and Gross, Herbert.** 5, s.l. : De Gruyter, 2019, Advanced Optical Techniques, Vol. 8, pp. 385–402.

23. *Optical design and specification of telecentric optical systems.* **Pate, Michael.** s.l. : Society of Photo-Optical Instrumentation Engineers, 1998. Proceedings of SPIE. Vol. 3482, pp. 877 - 886.

24. **Dilworth, Donald.** *Lens Design: Automatic and quasi-autonomous computational methods and techniques.* [ed.] R. Barry Johnson. Bristol : IOP Publishing Ltd, 2018.

25. *Integrated opto-mechanical tolerance analysis.* **Lamontagne, Frédéric, et al.** [ed.] José Sasián and Richard N. Youngworth. s.l. : Society of Photo-Optical Instrumentation Engineers, 2022. Proceedings of SPIE. Vol. 12222.